New Phytologist

Research

The StPti5 ethylene response factor acts as a susceptibility factor by negatively regulating the potato immune response to pathogens

Anna Coll[1], Tjaša Lukan[1], Katja Stare[1], Maja Zagorščak[1], Tjaša Mahkovec Povalej[1], Špela Baebler[1], Salomé Prat[2], Núria Sánchez Coll[2], Marc Valls[2,3], Marko Petek[1] and Kristina Gruden[1]

[1]Department of Biotechnology and Systems Biology, National Institute of Biology, Ljubljana, 1000, Slovenia; [2]Centre for Research in Agricultural Genomics (CSIC-IRTA-UAB-UB), Bellaterra, 08193, Catalonia, Spain; [3]Department of Genetics, Microbiology and Statistics, Universitat de Barcelona, Barcelona, 08028, Catalonia, Spain

Authors for correspondence:
Kristina Gruden
Email: kristina.gruden@nib.si

Tjaša Lukan
Email: tjasa.lukan@nib.si

Received: *27 February 2024*
Accepted: *2 July 2024*

New Phytologist (2024)
doi: 10.1111/nph.20004

Key words: ethylene response factor, immune signalling, potato virus Y (PVY), Pti5, *Ralstonia solanacearum*, *Solanum tuberosum* (potato), susceptibility factor.

Summary

- Ethylene response factors (ERFs) have been associated with biotic stress in Arabidopsis, while their function in non-model plants is still poorly understood. Here we investigated the role of potato ERF StPti5 in plant immunity.
- We show that StPti5 acts as a susceptibility factor. It negatively regulates potato immunity against potato virus Y and *Ralstonia solanacearum*, pathogens with completely different modes of action, and thereby has a different role than its orthologue in tomato. Remarkably, StPti5 is destabilised in healthy plants via the autophagy pathway and accumulates exclusively in the nucleus upon infection. We demonstrate that StEIN3 and StEIL1 directly bind the *StPti5* promoter and activate its expression, while synergistic activity of the ethylene and salicylic acid pathways is required for regulated *StPti* expression.
- To gain further insight into the mode of StPti5 action in attenuating potato defence responses, we investigated transcriptional changes in salicylic acid deficient potato lines with silenced *StPti5* expression. We show that StPti5 regulates the expression of other ERFs and downregulates the ubiquitin-proteasome pathway as well as several proteases involved in directed proteolysis.
- This study adds a novel element to the complex puzzle of immune regulation, by deciphering a two-level regulation of ERF transcription factor activity in response to pathogens.

Introduction

Plants depend on a multi-layered immune system to recognise and fight off different attackers (Zhou & Zhang, 2020; Yuan *et al.*, 2021b). A first layer of active plant innate immunity is induced by conserved microbial- or pathogen-associated molecular patterns (MAMPs or PAMPs) recognised by transmembrane pattern recognition receptors (PRRs) initiating the PAMP-triggered immunity (PTI) response (Boller & Felix, 2009). Effector-triggered immunity (ETI) is the second and more specific defence layer, often associated with hypersensitive response (HR)-conferred resistance. In ETI, the microbial effectors are directly or indirectly recognised by specific intracellular nucleotide-binding/leucine-rich-repeat (NLR) receptors (Cui *et al.*, 2015). Both PTI and ETI layers function synergistically and share several signalling regulators, to ensure a robust response of immunity (Ngou *et al.*, 2021; Yuan *et al.*, 2021a). Shared pathways include mitogen-activated protein kinase (MAPK) cascades, calcium response, reactive oxygen species burst and hormonal signalling, which finally lead to a transcriptional reprogramming of cells (Yuan *et al.*, 2021b). This last step requires a coordinated function of different transcription factors (TFs), among which AP2/ERF, bHLH, NAC, TGA/bZIP and WRKY are shown to play prominent roles (Tsuda & Somssich, 2015; Birkenbihl *et al.*, 2017).

Ethylene response factor (ERF) TFs are members of the large AP2/ERF family and are defined by the presence of a single AP2/ERF DNA interaction domain. This domain is composed of 60 amino acids that form a 3D structure consisting of a three-stranded anti-parallel β-sheet and an α-helix packed approximately parallel to the β-sheet (Allen *et al.*, 1998). ERFs are characterised by the presence of conserved alanine and aspartic acid at positions 14 and 19, respectively (Sakuma *et al.*, 2002). They were shown to specifically bind an AGCCGCC motif designated as GCC-box which is found in the promoters of many jasmonic acid (JA)/ethylene inducible pathogenesis-related (PR) genes (Ohme-Takagi & Shinshi, 1995).

Several members of the ERF family, mostly belonging to group IX (Nakano *et al.*, 2006), have been linked to biotic stress

responses in Arabidopsis (Huang *et al.*, 2015). AtERF1 and ORA59, for instance, confer resistance to several necrotrophic fungi (Berrocal-Lobo *et al.*, 2002; Berrocal-Lobo & Molina, 2004; Pré *et al.*, 2008) by acting downstream of the intersection between ethylene and JA pathways (Lorenzo *et al.*, 2003; Pré *et al.*, 2008; Zarei *et al.*, 2011). Moreover, ORA59 is shown to act as a key node of salicylic acid (SA) and JA antagonistic crosstalk (Van der Does *et al.*, 2013). The involvement of ERFs in disease resistance against bacteria, fungi and viruses has also been documented in crops (Feng *et al.*, 2020). In soybean (*Glycine max*), the GmERF5 and GmERF113 ERF TFs were shown to play key roles in defence response to *Phytophthora sojae* (Dong *et al.*, 2015; Zhao *et al.*, 2017), while in Chinese wild grapevine (*Vitis pseudoreticulata*) VpERF2 and VpERF3 enhanced resistance to both the biotrophic bacterial pathogen *Ralstonia solanacearum* and the oomycete *Phytopthtora parasitica* (Zhu *et al.*, 2013). In tomato, ERF TFs SlPti4, SlPti5 and SlPti6 have been shown to be involved in disease resistance against several pathogens. They were identified as interacting partners of the R gene Pto product and were then characterised as TFs that recognise the promoter region of genes encoding pathogenesis-related (PR) proteins (Zhou *et al.*, 1997). Based on these findings, Zhou suggested they were probable components linking an R gene product to the expression of specific defence-related genes (Zhou *et al.*, 1997). Overexpression of *SlPti5* was shown to enhance resistance to *Pseudomonas syringae* pv. tomato, a hemi biotrophic bacteria causing the tomato bacterial speck disease (He *et al.*, 2001) and it was also linked to aphid resistance in tomato (Wu *et al.*, 2015). Later on, SlPti4 and SlPti6 were also shown to promote plant defence against pathogenic bacteria (Gu *et al.*, 2002; Wang *et al.*, 2021). A Pti5 orthologue that could improve resistance to *Verticillium dahliae* has recently been identified in wild eggplant (*Solanum torvum* Sw.) (Li *et al.*, 2023).

In contrast to these positive regulators, a few ERF TFs with a transcriptional repressive function have been identified to increase plant susceptibility to different pathogens. Among them, AtERF4 was found to decrease resistance to the necrotrophic fungus *Fusarium oxysporum* in Arabidopsis, while StERF3 negatively regulates resistance to the hemi biotroph *Phytophthora infestans* in potato (Tian *et al.*, 2015). VpERF1 can enhance susceptibility to *R. solanacearum* and *P. parasitica* in grapevine (Zhu *et al.*, 2013) and OsERF922 to *Magnaporthe oryzae* in rice (Liu *et al.*, 2012). However, despite the importance of ERFs in biotic stress responses, the function of most of them remains unknown, especially in crops.

Here we aimed to elucidate the function of the ERF transcriptional network in potato immune responses. Potato (*Solanum tuberosum* L.) is the fourth most important crop in the world. It is grown on a significant scale in 130 countries, with a gross production value of 63.6 billion US dollars in 2016, and a yearly production of 368 million tons in 2018 (Dolničar, 2021). We show that StPti5, the potato orthologue of SlPti5, that lacks a corresponding Arabidopsis orthologue, acts as a susceptibility factor in potato. We further deciphered its regulation on transcriptional and protein stability levels as well as identified its downstream targets.

Materials and Methods

Plant material

Two potato (*Solanum tuberosum* L.) genotypes were used in this study including the nontransgenic cultivar Rywal (nontransgenic, NT), which shows hypersensitive response (HR)-conferred resistance to potato virus Y (PVY), and its transgenic line, expressing *NahG* and thus impaired in SA accumulation (SA reduced to < 10% of native values; NahG) and sensitive to PVY (Baebler *et al.*, 2014). Potato plants were grown in stem node tissue culture in long day conditions at 22°C. Two weeks after node segmentation, they were transferred to soil and kept in growth chambers under controlled environmental conditions of 22°C, 16 h : 20°C, 8 h, light : dark, with a light intensity of 4000 lm m^{-2} and 60–70% relative humidity. *Nicotiana benthamiana* Domin plants were grown from seeds and kept in growth chambers under the same controlled conditions.

Hormonal treatments

For all treatments, 4-wk-old potato plants were used. SA treatments were performed by spraying plants with 300 μM INA (98% 2,6-Dichloroisonicotinic acid, Aldrich) in 1% ethanol. For ethylene and methyl jasmonate (MeJA) treatments, plants were sealed in airtight containers and treated with 50 ppm ethylene or 0.25 μl MeJA (95% Methyl Jasmonate, Aldrich) per l of air. Control plants were sealed in airtight containers with no treatment or sprayed with the corresponding mock solution (Supporting Information Dataset S1).

To inhibit ethylene signalling pathway, plants were treated with SmartFresh (AgroFresh, Inc.) containing 0.14% 1-Methylcyclopropene (1MCP) in airtight containers. To effectively release 1MCP, the treatment was performed according to the protocol provided by the manufacturer, with an estimated application rate of 1000 ppb (v/v) 1MCP. After 2 h of incubation, the sealed container was opened, plants were treated with the corresponding hormones and a new bottle containing dissolved 1MCP was placed in the container.

Leaves were harvested 24 h after treatments and immediately frozen in liquid nitrogen (Dataset S1).

DNA constructs

The full length *StPti5* (Sotub02g020180; GenBank: XM_006367134) cDNA was amplified from NT and cloned by Gateway into the β-estradiol inducible vector containing GFP (pABinGFP; Bleckmann *et al.*, 2010), to obtain the pABinGFP_StPti5 construct.

Nested PCR was performed to amplify the upstream region of *StPti5*, 1 kb in front of the start codon, out of the NT genomic DNA. The amplified fragments were cloned into the pJET plasmid using the CloneJET PCR Cloning Kit (Thermo Scientific) and used for further promoter analyses. The NT1 promoter sequence (GenBank: OR750856) was introduced into the Y1H pAbAi plasmid Clontech Laboratories, Inc. (Takara Bio USA,

Inc., Mountain View, CA, USA), via restriction enzyme digestion. A 66 bp long oligonucleotide fragment containing four tandem copies of the GCC-box (GCC) and its mutated version (GCCmut) (Wang *et al.*, 2015) were also cloned into the Y1H vector. The same oligonucleotide fragments fused to a minimal promoter (Ow *et al.*, 1987) and the NT1 promoter sequence were likewise cloned by Gateway into the pGWB435 LUC reporter plasmid (Nakagawa *et al.*, 2007).

The coding sequences of *NAC domain-containing protein 55* (*StANAC55*, GenBank: OR736059), *MYC2 transcription factor* (*StMYC*, GenBank: OR736060), *ETHYLENE INSENSITIVE 3* (*StEIN3*, Sotub01g034310), *EIN3-like 1* (*StEIL1*, GenBank: OR736061), *EIN3-like 2 (StEIL2*, GenBank: OR736062), *StPti5*, *TGACG-motif binding factor 2.3* (*StTGA2.3*, OM569619 (Tomaž *et al.*, 2023)), *TGA2.2* (*StTGA2.2*, OM569618 (Tomaž *et al.*, 2023)) and *TGA2.1* (*StTGA2.1*, OM569617 (Tomaž *et al.*, 2023)) were amplified from NT and cloned into the yeast pGADT7 vector Clontech Laboratories, Inc. (Takara Bio USA, Inc.). *StMYC2*, *StEIL1*, *StEIL2*, *StEIN3*, *StPti5* were additionally cloned into pABinGFP (Bleckmann *et al.*, 2010) using Gateway® LR Clonase TM II Enzyme Mix (Invitrogen).

For silencing experiments, a part of *StPti5* gene was amplified from NT and introduced into pH7GWIWG2(II) (Karimi *et al.*, 2002) using Gateway technology as explained in Lukan *et al.* (2020).

All constructs were verified by Sanger sequencing (Eurofins Genomics, Ebersberg, Germany; Sanger *et al.*, 1977; Smith *et al.*, 1986). Primers and double stranded oligonucleotides used are listed in Table S1.

Pathogen inoculation and disease resistance evaluation

PVYN605, tagged with green fluorescent protein (PVY N605-GFP) or PVYNTN (isolate NIB-NTN, AJ585342) (Jakab *et al.*, 1997) were used to inoculate 4 wk-old plants as described by Baebler *et al.* (2009).

A constitutively luminescent Pps-lux variant of *Ralstonia solanacearum* UY031, a highly aggressive strain on potato (Cruz *et al.*, 2014) was used in all experiments. Plants were inoculated by soil drenching after mild root disruption with a 1 ml tip using 40 ml of a 10^8 CFU ml^{-1} bacterial suspension per pot as described (de Pedro-Jové *et al.*, 2021). Plants were kept in the inoculation chamber (27°C, 12 h : 12 h, dark : light) and symptoms were recorded over time using a 1–4 scale (1 = 25% wilting, 4 = 100% wilting). Bacterial luminescence was used to quantify bacterial loads in stem samples (Cruz *et al.*, 2014). Briefly, 0.5 cm long stem sections were excised and incubated for 30 min into a sterile 2 ml tube with 200 µl of sterile distilled water and luminescence was measured on a luminometer (FB 12; Berthold Detection Systems, Bad Wildbad, Germany).

Agroinfiltration of *Nicotiana benthamiana*

Three-wk-old *N. benthamiana* plants were used for transient transformation. Constructs were introduced into electrocompetent *Agrobacterium tumefaciens* GV3101 by electroporation and effective transformation confirmed by colony PCR (KAPA2G Robust HotStart; Kapa Biosystems, Inc., Roche, Wilmington, MA, USA) (Table S1), following our previous procedures (Lukan *et al.*, 2018b). Cultures of the transformed cells were infiltrated into the 2nd and 3rd fully developed bottom leaves of *N. benthamiana* plants as reported previously (Lukan *et al.*, 2018b). *Agrobacterium* transformed with silencing suppressor p19 (kindly provided by Prof. Jacek Hennig) was added to the mixture at 1 : 1 ratio for the transactivation experiments. Empty *A. tumefaciens* GV3101 was used as a control. For colocalisation studies, *Agrobacterium* transformed with nucleus marker H2B protein tagged with red fluorescent protein (H2BRFP) (Lukan *et al.*, 2018b) was added to the mixture at 1 : 1 ratio. For experiments on PVY-infected plants, agroinfiltration was performed 7 d postinfection (dpi).

Generation of *StPti5* silenced transgenic potato plants

To obtain transgenic potato plants silenced for *StPti5* expression (shPti5 NahG), the short hairpin RNA (shRNA) construct pH7GWIWG2_shPti5 was introduced into *A. tumefaciens* LBA4404 by electroporation as in Lukan *et al.* (2018b). The transformed cells were used for stable transformation of NahG as described previously (Lukan *et al.*, 2023) using appropriate selection media.

Gene expression analysis by quantitative PCR

Potato leaf samples (*c.* 150 mg) were homogenised using FastPrep instrument (MP Biomedicals, Santa Ana, CA, USA). Total RNA was isolated using RNeasy Plant Mini kit (Qiagen), treated with 1.3 U DNase I (Qiagen) per µg of RNA, while reverse transcription and quantitative polymerase chain reaction were performed as described previously (Lukan *et al.*, 2020). For the analysis of *StPti5*-silenced plants, data obtained on ViiA 7 or 7900HT Fast Real-Time PCR instrument (Applied Biosystems, Thermo Fisher Scientific corporation, Waltham, MA, USA) was normalised to *cytochrome oxidase* (*COX*). In case of hormonal treatment experiments, the expression of *StPti5*, *pathogenesis-related protein 1b (StPR1b)*, *potato cysteine proteinase inhibitor family 8.3 (StCPI8.3)*, and *aminocyclopropanecarboxylate oxidase 4 (StACO4)* were followed via high-throughput quantitative polymerase chain reaction (Fluidigm BioMark™ HD System Real-Time PCR, Fluidigm) and data was normalised to two endogenous control genes, *COX* and *elongation factor 1α* (*EF-1*). Preamplification of cDNA and gene expression analysis using Fluidigm BioMark™ HD System Real-Time PCR (Fluidigm) were performed as described before (Ramšak *et al.*, 2018). quantGenius (Baebler *et al.*, 2017) was used for relative gene expression quantification based on the standard curve method. Welch's *t*-test with the Holm–Bonferroni method, to control the family-wise error rate (FWER) on $\log_2$ transformed data scaled to control mean, was used to determine differentially expressed genes. For primer and probe information and full experimental details, see Table S2, Datasets S1 and S2.

RNA-Seq analysis

NahG and shPti5 NahG plants were sampled 3 d after mock- or PVY N605-GFP- inoculation (Dataset S2), and total RNA was isolated as described above, followed by cleaning step using RNeasy MinElute Cleanup Kit (Qiagen). Stranded RNA-Seq library preparation and HiSeq4000 100 bp paired-end sequencing (Illumina) were performed by SeqMatic LLC using standard Illumina protocols. Read quality control was performed using FastQC (Babraham Bioinformatics, The Babraham Institute, Cambridge, UK) and further read analysis (merging of overlapping pairs, mapping of reads to the potato genome and read counting) was done in CLC Genomics v.9.1 (Qiagen) (Methods S1). For differential expression (DE) analysis, we used two approaches, using either CLC Genomics or R, as explained in detail in Methods S1. Adjusted *P*-values < 0.05 were considered statistically significant.

Yeast one-hybrid assay

Yeast one-hybrid (Y1H) assays were conducted using Matchmaker Gold One-hybrid technology (Clontech) as described by the manufacturer. To create the bait reporter strain, the Y1H Gold strain was transformed with the linearised pABAi plasmid containing the promoter of interest using the polyethylene glycol/LiAc-based method. After selection on SD/-Ura agar medium and confirmation of the bait sequence integration by colony PCR, the colonies were used for further transformation with the pGADT7 constructs containing the TFs of interest. SD media without Leucin (SD/Leu) was used as control media for transformation. Positive interactions were selected on SD/Leu agar plates containing aureobasidin A (Aba).

Transactivation assay

To study protein–DNA interactions *in planta*, we performed transient transactivation studies according to Lasierra & Prat (2018). Leaf discs of *N. benthamiana* plants co-expressing the promoter LUC reporter and β-estradiol inducible effector cassettes, in combination with p19 (as mentioned in the previous section), were sampled 3 d postagroinfiltration (dpa). The collected discs were placed in microplate reader wells that contained 175 µl of 4 mg ml^{-1} d-luciferin per 50 ml Murashige & Skoog basal salt mixture solution. For effector construct activation, β-estradiol was added to a final concentration of 10 µM. No inducer was added to half of the leaf discs, used as controls for basal activity. For each effector, 18 replicates and two independent experiments were performed. Luminescence activity was recorded in the luminometer microplate reader LB960 (Berthold Technologies, Bad Wildbad, Germany) *c.* every 30 min for at least 24 h. Measurements were transformed to $\log_{10}$, and within each time point, Wilcoxon signed-rank tests with Benjamini–Hochberg procedure (v.0.7.2, Kassambara, 2023a) for false discovery rate (FDR) was used to compare β-estradiol-treated vs nontreated samples. Data was visualised using R (R Core Team, 2023) packages ggplot2 (v.3.4.2, Wickham, 2016) and ggpubr (v.0.6.0, Kassambara, 2023b).

Western blot

Nicotiana benthamiana leaves previously transformed with the StPti5_GFP fusion under β-estradiol inducible promoter (StPti5-GFP) or with p19 only, were collected 50 h or 76 h after the corresponding chemical treatment (to be described later). Proteins were extracted and StPti5-GFP was pulled down and eluted (see Methods S2 for details). After trapping, StPti5-GFP was analysed by SDS-PAGE and western blot using anti-GFP polyclonal antibodies (1 : 5000; Thermo Fisher Scientific) and secondary antibodies (1 : 5000; Anti-Rabbit IgG (H + L), HRP conjugated, Promega) (Methods S2). Chemiluminescence was detected using Clarity Max Western ECL substrate (Bio-Rad). Images were acquired by UVP ChemStudio system (Analytik Jena, Jena, Germany).

Chemical treatments

To induce pABinGFP_StPti5 construct *in planta*, *N. benthamiana* leaves were sprayed with 10 µM β-estradiol 3dpa. At the same time, the treated leaves were also infiltrated with 5 mM 3-methyladenine (3-MA) or 100 µM MG132 diluted in DMSO. Control plants were infiltrated with 0.5% DMSO. Experimental details are shown in Dataset S3.

Confocal microscopy

The presence of the fused fluorescence proteins was visualised on the abaxial side of detached infiltrated leaves with confocal microscopes Leica TCS SP5, Leica TCS LSI and Leica Stellaris 5 as explained in Methods S3.

Images are presented as maximum projections from Z-stacks. Z-stack size was adjusted to 10 steps to cover *c.* 50 µm of the tissue. Image overlay of the brightfield with all channel's maximum projections from Z-stacks, in the case of Leica TCS SP5, or image overlay of all channel's maximum projections from Z-stacks, in the case of Leica TCS LSI, was performed using Leica Las AF Lite software (Leica Microsystems, Wetzlar, Germany).

Bioinformatic analysis

Potato ERF genes were previously identified by Charfeddine *et al.* (2014) based on the potato gene model provided by The Potato Genome Consortium (PGSC) (Potato Genome Sequencing Consortium, 2011). We used orthologue information included in GoMapMan (Ramsak *et al.*, 2013) to link each ERF group IX gene with identifiers from the ITAG gene model (The Tomato Genome Consortium, 2012), as well as with information from Potato Oligo Chip Initiative (POCI) (Kloosterman *et al.*, 2008).

Heatmap presenting $\log_2$FC (adjusted *P*-value < 0.05) of previous microarray dataset (Baebler *et al.*, 2014) was generated

using R (R Core Team, 2023) package GPLOTS (v.3.1.3, Warnes *et al.*, 2022). In case one gene was targeted by more than one POCI probe, the most responsive POCI was prioritised to represent the corresponding *StERF* gene.

The amino acid sequences of ERF-IX from Arabidopsis (Nakano *et al.*, 2006), tomato (*Solanum lycopersicum* L.) (Sharma *et al.*, 2010; Pirrello *et al.*, 2012) and ERF-IX potato genes (Charfeddine *et al.*, 2014) retrieved in our gene expression dataset were used to build a phylogenetic tree. To determine the optimal number of sequence clusters, affinity propagation clustering (v.1.4.10, Bodenhofer *et al.*, 2011) was conducted on mutual pairwise similarities obtained through protein length scaled Levenshtein distances (v.0.9.10, van der Loo, 2014). Circular dendrogram was constructed using the R package DENDEXTEND (v.1.17.1, Galili, 2015).

The location of the selected *StPti5* potato ERF gene (Sotub02g020180) within the potato genome and the sequence of its promoter region were obtained from the *S. tuberosum* Group Phureja DM1-3 v4.03 genome assembly (Potato Genome Sequencing Consortium, 2011). Multiple sequence alignment of 1000 bp long promoter sequences was performed using CLC Main Workbench 6.8.1 and MUSCLE algorithm. Analyses of transcription factors binding sites in the 1600–1900 bp long promoter regions were performed using TRANSFAC (Biobase) and FOOTPRINTDB (Sebastian & Contreras-Moreira, 2014).

Results

Differential regulation of potato ERF transcription factors during the immune response to potato virus Y

Given that group IX ERF genes have been particularly associated with plant defence responses (Nakano *et al.*, 2006), we investigated the expression profile of members of this subfamily in potato. We first examined transcript levels of these genes in potato response to PVY, one of the viruses leading to the most significant potato losses world-wide (Kreuze *et al.*, 2020) in our previous dataset that included the cv Rywal (nontransgenic, NT), harbouring the *Ny-1* gene and showing HR-conferred resistance, and its susceptible transgenic counterpart deficient in SA (NahG) (Baebler *et al.*, 2014). Sixteen genes of the *StERF-IX* group (Charfeddine *et al.*, 2014), corresponding to 26 POCI microarray probes, were identified on the microarray. Indeed, 14 genes were observed to be differentially expressed after PVY infection, in at least one of the experimental conditions (Fig. 1a), supporting the importance of this gene family in potato immunity. In NT plants, 5 out of 6 differentially expressed genes were downregulated at 1 dpi, while most of them were upregulated at 3 and 6 dpi (Fig. 1a). By contrast, in NahG plants none of these genes showed a differential expression or they were only weakly upregulated at 1 dpi, while displayed a strong induction from 3 dpi onwards (Fig. 1a).

The strongest response among the *ERF-IX* genes, was shown for *Sotub09g019370*, *Sotub02g020180* and *Sotub02g023760* (Fig. 1a). *Sotub02g020180* is, in the *S. tuberosum* group Phureja DM1-3 genome annotated as pathogenesis-related gene transcriptional activator *Pti5* (Potato Genome Sequencing Consortium, 2011), and is an orthologue of tomato *Pti5* gene (Fig. S1). The gene has 549 base pairs (bp) of open reading frame (ORF) allowing for a protein of 182 amino acids (aa). Although it clustered with *AtERF*s from subgroup IXc, including *AtERF1*, *ORA59* and *AtERF14*, among others (Nakano *et al.*, 2006), no orthologues of *StPti5* were found in Arabidopsis (Fig. S1).

We next performed a more detailed spatial analysis of *StPti5* transcription factor, by following its expression levels in small tissue sections collected around the lesion (Fig. 1b). *StPti5* showed an induction peak in the area immediately surrounding the lesion (section A) of PVY-infected plants, while its expression decreased in both genotypes in the surrounding tissues (section B–D). Induction in the viral amplification area (section A) was at least two times stronger in NahG plants compared to NT plants (Fig. 1b). Strong induction in infected plants and its spatial regulation near the lesions thus suggests a role of *StPti5* in the immune response.

StPti5 negatively regulates potato immunity

To investigate the role of *StPti5* in potato immunity, lines silenced in *StPti5* gene expression were generated in the NahG genetic background (shPti5 NahG) (Fig. S2). The NahG genotype was selected for *StPti5* silencing because, in contrast to the fully resistant NT plants, SA deficiency of these plants enabled us to study function of this ERF in immunity. Lines were first tested for potato–PVY interaction, observing that *StPti5* silencing led to significantly lower viral RNA levels compared with NahG plants at 5 dpi (Fig. 2a), consistent with impaired *StPti5* expression delaying PVY multiplication in the inoculated leaves. We also monitored symptom development. The first necrotic lesions on the inoculated leaves were observed at 3 dpi in both genotypes. However, the number of lesions from 4 to 8 dpi was significantly lower in *StPti5*-silenced plants compared to NahG plants (Figs 2b, S3). Moreover, the first symptoms on the upper noninoculated leaves appeared at 11 dpi in all genotypes, although at later time points NahG plants displayed more severe systemic symptoms than *StPti5*-silenced plants (Fig. 2c). From these observations we can conclude that *StPti5* contributes to a more efficient initiation of viral infection, higher local spread of the virus and more severe systemic symptoms.

The function of potato *StPti5* has not been, to our knowledge, previously studied. However, *SlPti5* has been reported in tomato to enhance disease resistance to *P. syringae* pv *tomato* (He *et al.*, 2001; Wang *et al.*, 2021) and contribute to aphid (*Macrosiphum euphorbiae*) resistance (Wu *et al.*, 2015). Our data show the opposite role of the potato orthologue gene after PVY infection. We thus decided to explore whether the decreased susceptibility to PVY observed in *StPti5*-silenced plants was a specific response to the virus or it was also observed after infection with other pathogens, with a different mode of plant cell interaction, that is *R. solanacearum*, the most devastating potato bacterial pathogen and the causal agent of bacterial wilt (Mansfield *et al.*, 2012).

The role of *StPti5* in the response of potato against *R. solanacearum* was studied by following the development of wilting

New Phytologist

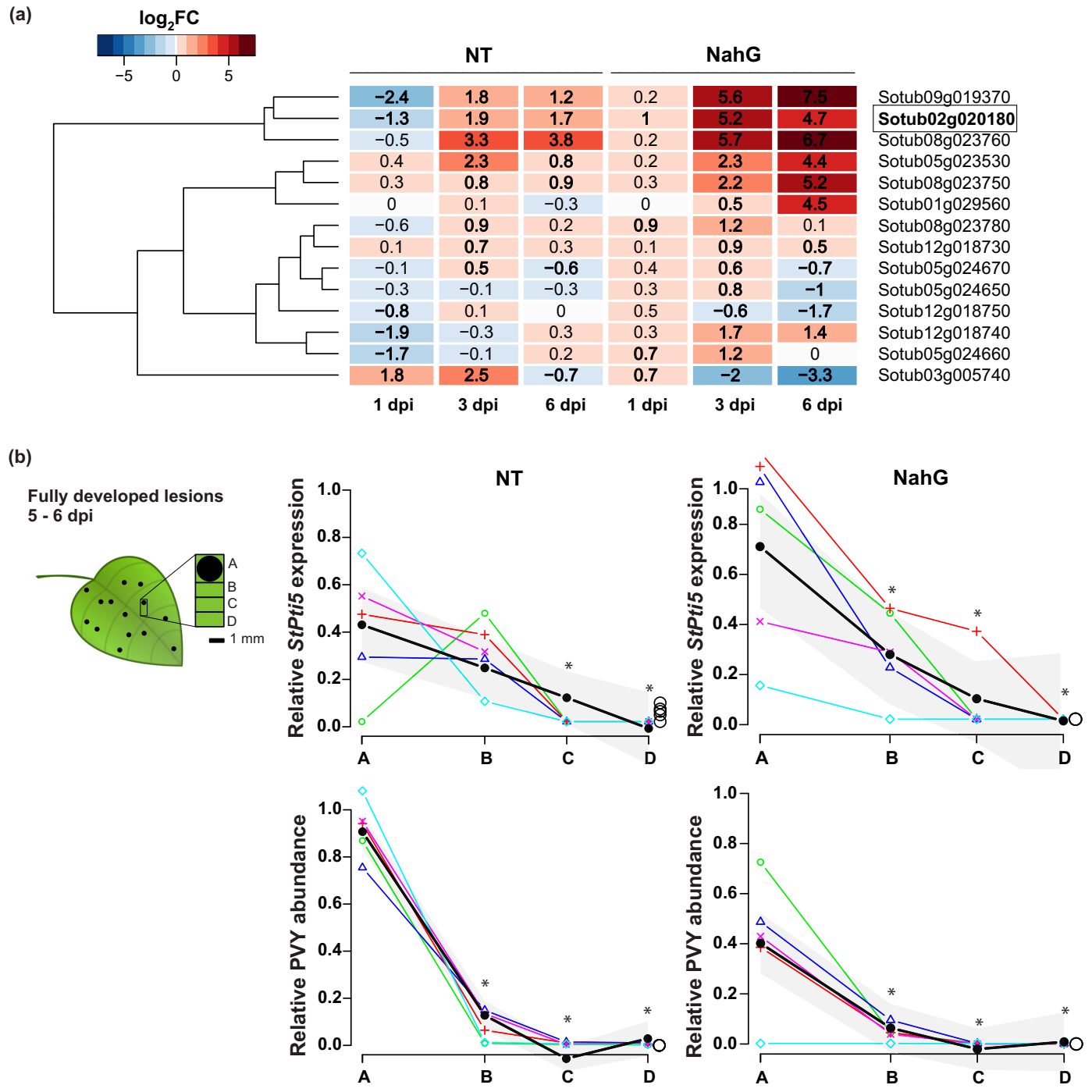

Fig. 1 ERFs gene expression in response to PVY infection. (a) Expression of *StERF-IX* genes in response to PVY. Heatmap reconstructed from our previous microarray dataset (Baebler *et al*., 2014). Log_2 fold changes (relative gene expression) of PVY-infected vs mock-inoculated plants of nontransgenic (NT) and salicylic acid deficient transgenic line (NahG) are shown for 1-, 3- and 6-d postinfection (dpi). Bold: statistically significant differences (FDR-adjusted *P*-value < 0.05). Framed: gene, selected for further analyses. (b) Spatial transcriptional regulation of *StPti5* (upper panel) and viral RNA (lower panel; data from Lukan *et al*., 2020) in NT and NahG plants inoculated with PVY. Tissue sections containing lesions (section A) and surrounding tissue (sections B, C and D) were sampled at 5–6 dpi, at the stage of fully developed lesions (scheme on the left, adapted from (Lukan *et al*., 2020)). Distance from the lesion, marked as positions A, B, C and D, is plotted on the *x*-axis and relative gene expression is plotted on the *y*-axis. Relative expression in mock-inoculated tissue sections is shown as empty circles at the end of *x*-axis. Asterisks denote the statistical significance (*P*-value < 0.05, 2nd order orthogonal polynomial contrasts) of differential gene expression at positions B, C and D, compared to position A. Spatial profile models are shown as thick black lines, with 95% confidence interval bands in grey. Relative gene expression values within individual lesions are presented with coloured symbols connected by a line.

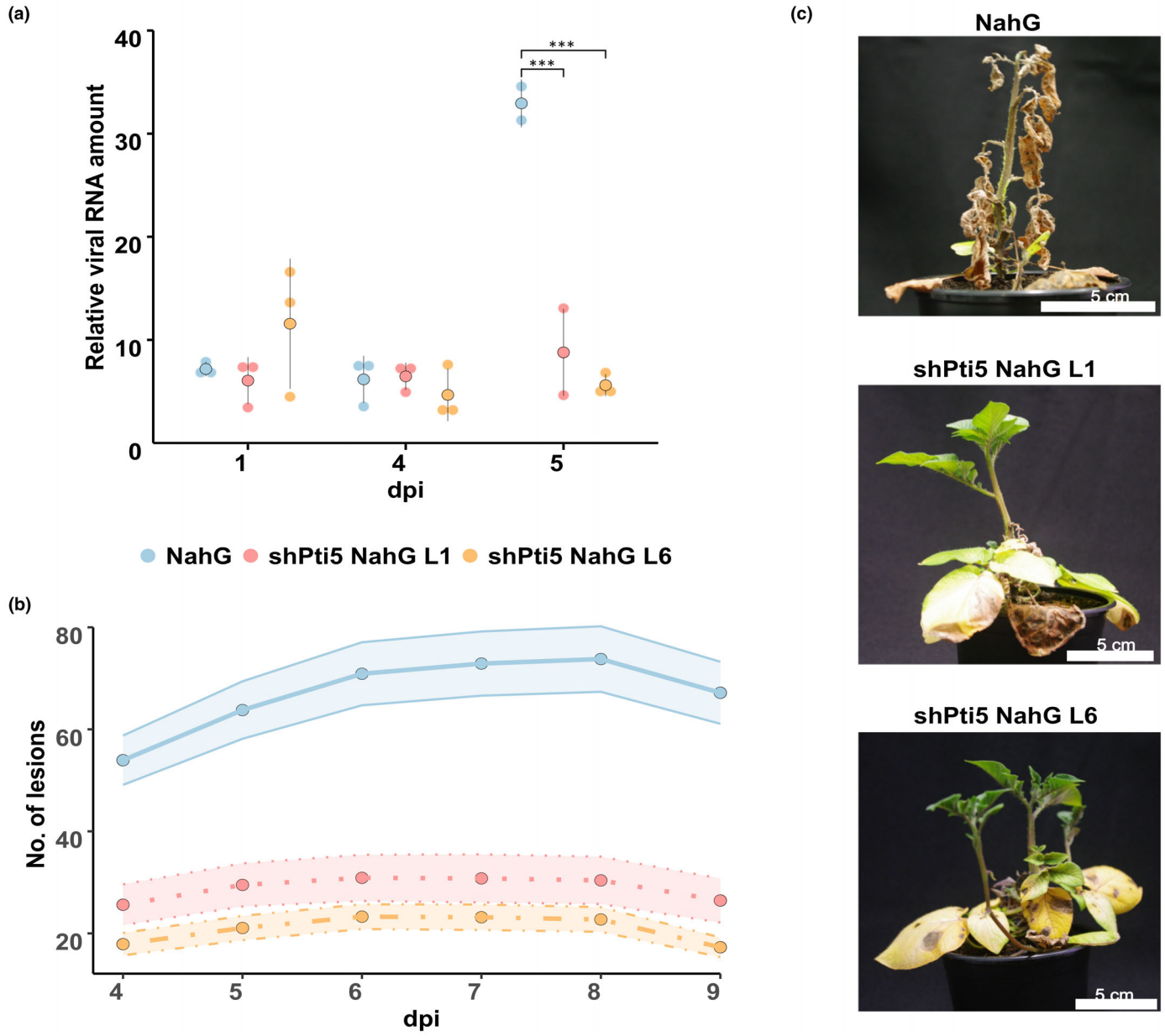

Fig. 2 *StPti5* increases potato susceptibility to PVY infection. (a) Relative abundance of viral RNA in PVY-inoculated leaves of NahG and two *StPti5*-silenced NahG lines (shPti5 NahG L1 and L6) at 1, 4 and 5 days postinfection (dpi). Arithmetic mean (full points) ± SD of three replicates (translucent points) are shown. Asterisks denote statistically significant differences between NahG and shPti5 NahG plants (Holm adjusted *P*-value *, < 0.05, **, < 0.01, ***, < 0.001) based on pairwise Welch's *t*-test. Order of visualization corresponds to the order of the items in the legend. (b) Number of lesions on PVY-inoculated leaves of NahG (full blue lines), shPti5 NahG L1 (sparse dotted pink lines) and shPti5 NahG L6 (dash-dotted orange lines). The average number of lesions (points) on 3 inoculated leaves ±SE of the mean (ribbon) as observed by 4–8 dpi are shown. Data correspond to 6 biological replicates. (c) Representative images of PVY-infected NahG, shPti5 NahG L1 and shPti5 NahG L6 at 47 dpi. The results were confirmed in two independent experiments (Supporting Information Fig. S3; Dataset S2).

symptoms after drench inoculation with a *R. solanacearum* luminescent reporter strain. We compared disease progress in NahG and *StPti5*-silenced NahG plants. Both potato genotypes showed a susceptible response, with the first symptoms appearing at 4 dpi. However, the disease index revealed that *StPti5* plays a negative role in the defence response of potato to *R. solanacearum* (Fig. 3). Symptoms were more pronounced in SA-deficient plants, while *StPti5* silencing reduced disease symptoms and delayed pathogen multiplication (Fig. 3; Dataset S4). This shows that *StPti5* increases potato susceptibility to *R. solanacearum*, same as for PVY.

StPti5 is a transcriptional activator

AP2/ERF domain factors were shown to a bind GCC-box elements (Ohme-Takagi & Shinshi, 1995). As expected from the

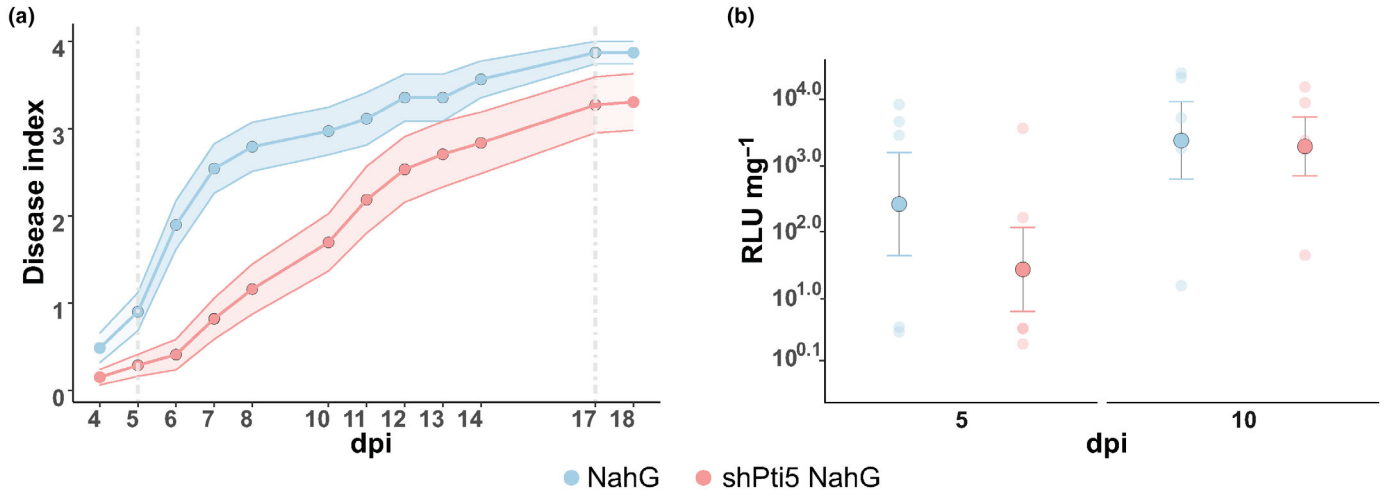

Fig. 3 *StPti5* increases susceptibility to bacterial pathogens *Ralstonia solanacearum*. (a) Progress of bacterial wilt measured in the salicylic acid (SA) deficient (NahG) and *StPti5*-silenced NahG (shPti5 NahG) plants at different days postinfection (dpi). Each measurement is presented as the mean (n NahG = 41; n shPti5 NahG = 33) disease index (0–4) ± SE of the mean (ribbon). Opaque shading denotes the region of statistically significant differences between NahG and shPti5 NahG plants. (b) Multiplication of bacteria in stem of different genotypes at 5 and 10 dpi. Results are presented as relative luminescence units per milligram of plant fresh tissue (RLU mg^{-1}, $\log_{10}$ transformed, translucent points), including mean (full points) ± SE of the mean (error bars) of 5 replicates.

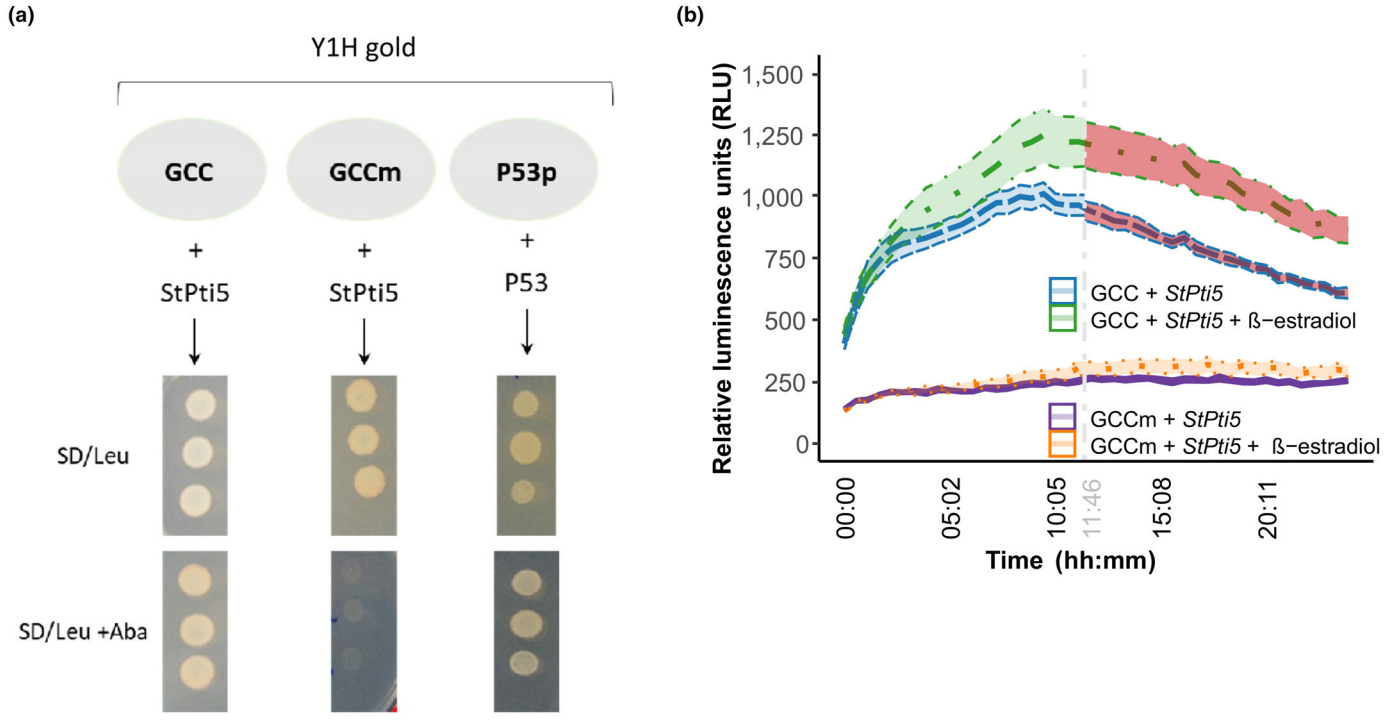

Fig. 4 StPti5 is a transcriptional activator binding the GCC-box for downstream gene activation. (a) Y1H analysis showing that StPti5 binds GCC-box *cis* element. The Y1H Gold strain containing four tandem repeat copies of GCC-box (GCC) can grow in the presence of aureobasidin A (Aba) only after co-expression of StPti5 bait construct. The same yeast strain containing a mutated version of the GCC-box (GCCm) does not grow in the presence of the Aba selective marker. P53 promoter (P53p) and P53 were used as a positive control. (b) Transactivation assays confirming that StPti5 is an activator. The β-estradiol inducible StPti5_GFP effector vector (StPti5) and the reporter construct expressing the firefly luciferase (*LUC*) gene under the GCC-box elements and a minimal promoter (GCC) were co-infiltrated in *Nicotiana benthamiana* leaves. Relative luminescence units (RLU) were measured over time in β-estradiol treated and untreated samples (green dash-dotted and blue dashed lines, respectively). A reporter construct containing the mutated GCC-box construct (GCCm) was used as a negative control (purple full and orange dotted lines). Significant differences between β-estradiol treated and untreated samples (FDR-adjusted *P*-value < 0.05; Wilcoxon signed-rank tests) are intensly shaded in pink and starting time of difference is marked with a vertical grey dashed line. The middle line connects the means (n = 12), while ribbon represents standard error of the mean.

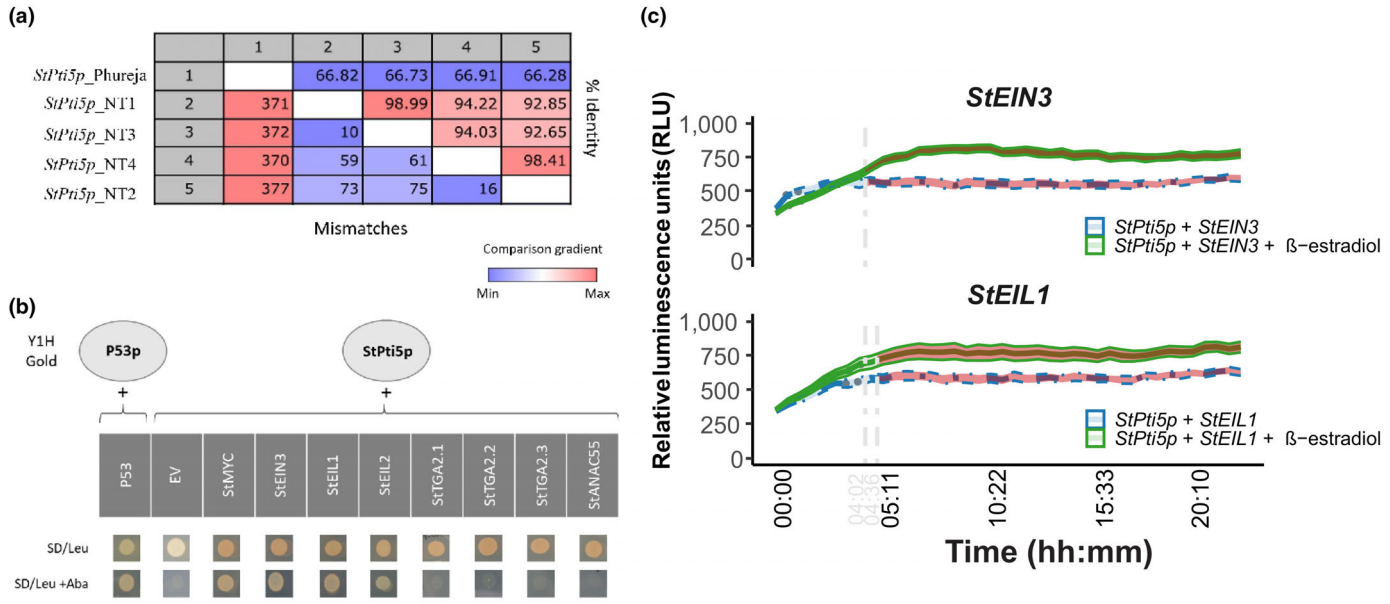

Fig. 5 EIN3-like transcription factors activate *StPti5* gene expression. (a) Pairwise comparison of 1000 bp *StPti5* promoter sequences. The table shows the % of identify (upper-right triangle) and the number of mismatches (lower-left triangle) between sequences, numbers are colour-shaded from minimum (blue) to maximum (red) values; (b) Y1H experiments showing that StMYC2 (OR736060), StEIN3 (Sotub01g034310), StEIL1 (OR736061) and StEIL2 (OR736062) bind the *StPti5* promoter. Y1H Gold yeast bearing the integrated *StPti5* (StPti5p) or P53 (P53p) promoter constructs were transformed with the selected transcription factors, as indicated. The aureobasidin A (Aba) yeast cell growth inhibitor was used as a screening marker. pAbAi_P53p/P53, positive control; the empty vector (EV)/*StPti5*p, negative control. The experiment was repeated twice. (c) Transient transactivation assays in *Nicotiana benthamiana* confirming the activation of *StPti5* by StEIN3 and StEIL1. The β-estradiol inducible StEIN3 (upper panel) or StEIL1 (lower panel) effector vectors and the *StPti5* promoter (StPti5p) fused to the firefly luciferase reporter were co-infiltrated in *N. benthamiana* leaves. Relative luminescence units (RLU) were measured over time in β-estradiol treated (green, full lines) and untreated (blue, sparse dash-dotted lines) samples. Significant differences between β-estradiol treated and untreated samples (FDR-adjusted *P*-value < 0.05) based on Wilcoxon signed-rank tests are intensly shades in pink and starting time of a difference is marked with a vertical grey dashed linefor StEIN3 and StEIL1, respectively. The middle line connects the means (n = 18), while ribbon represents standard error of the mean.

presence of a conserved AP2/ERF domain, Y1H experiments using a yeast strain containing a four tandem repeat GCC-box reporter confirmed that StPti5 binds this *cis* element (Fig. 4a). We further investigated functional interaction of StPti5 and the GCC-box in transient transactivation assays (Fig. 4b). *Nicotiana benthamiana* leaf discs expressing the firefly *LUC* gene under the GCC-box promoter construct showed an increase in luciferase (LUC) activity on expression of the β-estradiol inducible StPti5 effector (Figs 4b, S4), confirming that StPti5 binds the GCC-box and that it activates the expression of downstream genes.

StPti5 mediates crosstalk of ethylene and salicylic acid pathways

We further investigated the mechanisms regulating *StPti5* gene expression. Interestingly, we identified four different *StPti5* promoter variants in the Rywal (NT) genotype, indicating that StPti5 is encoded in this tetraploid cultivar by four distinct allelic forms (Dataset S5). Multiple sequence alignment and pairwise comparison of these promoters showed a high percentage of similarity, although 10–76 mismatches were observed within the 1 kb region upstream of the start codon. Moreover, these promoters share less than 67% of identity with the *StPti5* promoter sequence of *S. tuberosum* Group Phureja (Potato Genome Sequencing Consortium, 2011) (Fig. 5a).

In silico analyses of these promoter sequences identified conserved binding sites for multiple defence-related TFs (Dataset S5; Table S3). Among the candidates, we selected StANAC55, StMYC, StEIL1, StEIL2, StEIN3, StTGA2.3, StTGA2.2 and StTGA2.1 for further analysis. StMYC2, StEIN3, StEIL1 and StEIL2 were observed to bind the *StPti5* promoter in Y1H assay (Fig. 5b). We then conducted transient transactivation assays to confirm such interactions *in planta*. Only StEIN3 and StEIL1 increased the luciferase activity of the *StPti5* promoter construct, confirming that these factors activate *StPti5* gene expression (Figs 5c, S4).

These findings reveal that *StPti5* expression is induced by ethylene-responsive TFs. Previous studies on the effect of different hormonal treatments on *StPti5* gene expression had, however, shown this gene to be induced after SA application (Wiesel *et al.*, 2015). Therefore, we monitored *StPti5* transcript levels in NT plants, 24 h after different hormonal treatments, MeJA, the SA analogue INA and ethylene. *StPti5* was found to be induced between 1.5- and 2-fold after INA treatment, while no response was detected after other hormonal treatments (Figs 6, S5).

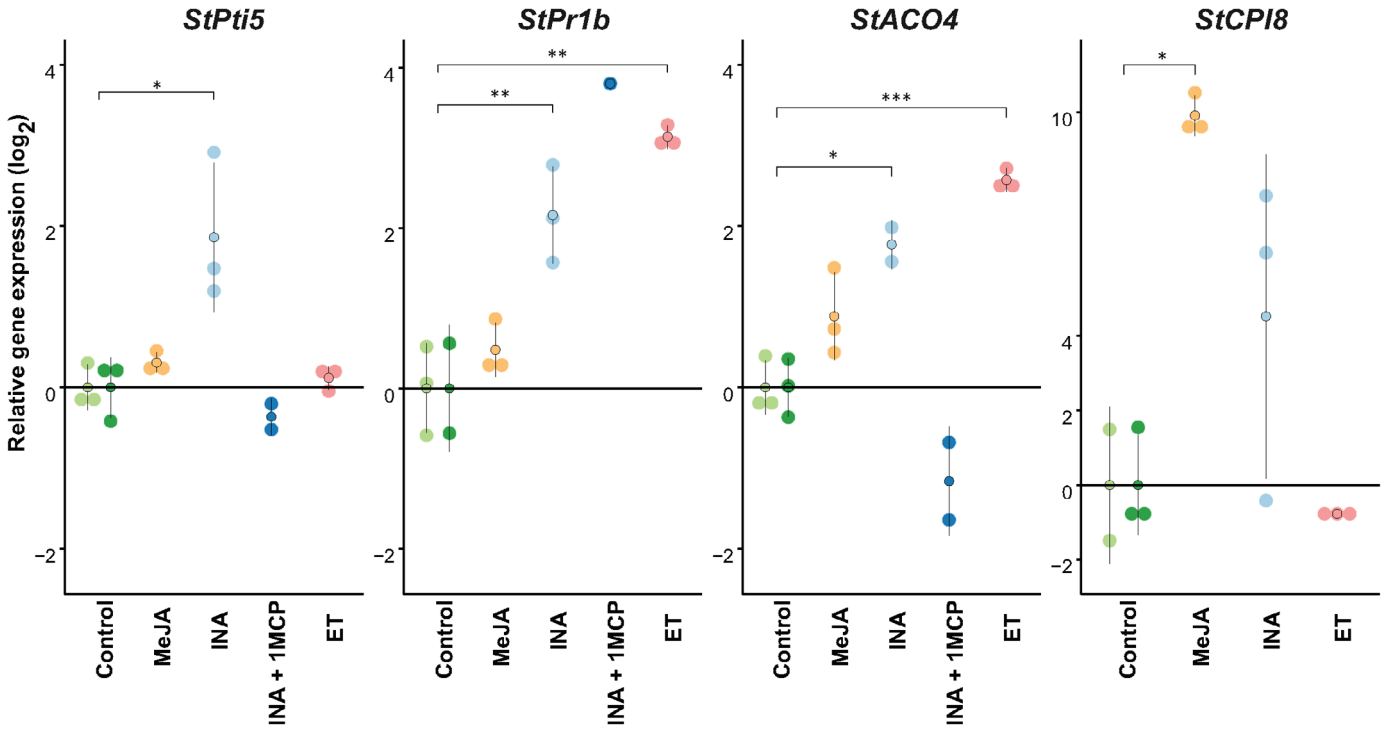

Fig. 6 SA activates *StPti5* expression in combination with ethylene signalling pathway. Leaves of nontransgenic potato plants were sampled 24 h after treatment with methyl jasmonate (MeJA), the SA analogue 2,6-dichloroisonicotinic acid (INA), INA and 1-Methylcyclopropene (INA + 1MCP) and ethylene (ET). Values are shown as $\log_2$ and scaled to the mean of the corresponding control (separate for INA/MeJA and ET treatments, marked with light and dark green, respectively). Arithmetic mean (full points) ± SD of three replicates (translucent points) are shown. Asterisks indicate significant differences between treated and untreated samples (Holm adjusted *P*-value, *, < 0.05, **, < 0.01, ***, < 0.001) based on Welch's *t*-test, as observed for *StPti5* (target gene), *StPR1b* (SA signalling marker), *StACO4* (ethylene signalling marker) and *StCPI8* (jasmonic acid signalling marker). For full experimental details, see Supporting Information Dataset S1. Results of an independent experiment are provided in Fig. S5.

Given that our results had demonstrated an interaction of the ethylene-responsive TF with *StPti5* promoter, we further investigated the involvement of ethylene signalling in *StPti5* expression. To this aim, we performed the INA treatment on plants previously treated with 1MCP which suppresses ethylene signalling pathway by blocking the ethylene receptors. We observed that the *StPr1b* SA marker was induced by INA treatment independently of the presence of 1MCP. By contrast, inhibition of the ethylene pathway strongly decreased response of *StPti5* to INA treatment (Figs 6, S5).

These results confirmed that *StPti5* is regulated via the SA signalling pathway, while showing, for the first time, that an active ethylene pathway is required for the activation of this gene.

The StPti5 protein is degraded in healthy plants by the autophagy pathway

To get more insight into the function of StPti5, we determined its subcellular localisation. We first checked its accumulation in healthy plants but observed that the signal of StPti5-GFP fluorescence was very weak. Thus, we further checked its accumulation after viral infection. Notably, following PVY inoculation, StPti5-GFP was strongly accumulated in both nuclei and cytoplasm of *N. benthamiana* leaves (Figs 7a, S6). Differences in StPti5 protein levels were confirmed by western blot (Figs 7b, S6, S7), where StPti5-GFP could not be detected in healthy plants. Nevertheless, analyses of the corresponding transcript showed them to be equivalent in healthy and infected plants (Table S4), hence indicating PVY infection increases the stability of the protein, while it is rapidly degraded in healthy plants.

To confirm these findings and further investigate which proteolytic pathway is responsible for StPti5 degradation, we treated agroinfiltrated plants with 26S proteasome inhibitor MG132 or the autophagy inhibitor 3-MA. Inhibition of the autophagy pathway resulted in StPti5-GFP detection in both mock- and PVY-inoculated plants, detected as Pti5-GFP fluorescence signal by confocal imaging and stronger bands on western blot, although protein abundance was still higher in PVY-infected plants (Fig. 7c,d). On the other hand, mock-inoculated plants treated with MG132, similarly to untreated mock plants, showed very weak fluorescent signal (Fig. S6), not allowing protein detection by western blot (Fig. 7d). Altogether, the data show that StPti5, if produced in healthy plants, is rapidly degraded via the autophagy pathway.

StPti5 causes transcriptional repression of protein degradation

To further investigate the function of StPti5 we compared the transcriptomes of PVY-infected NahG and *shPti5*-silenced NahG

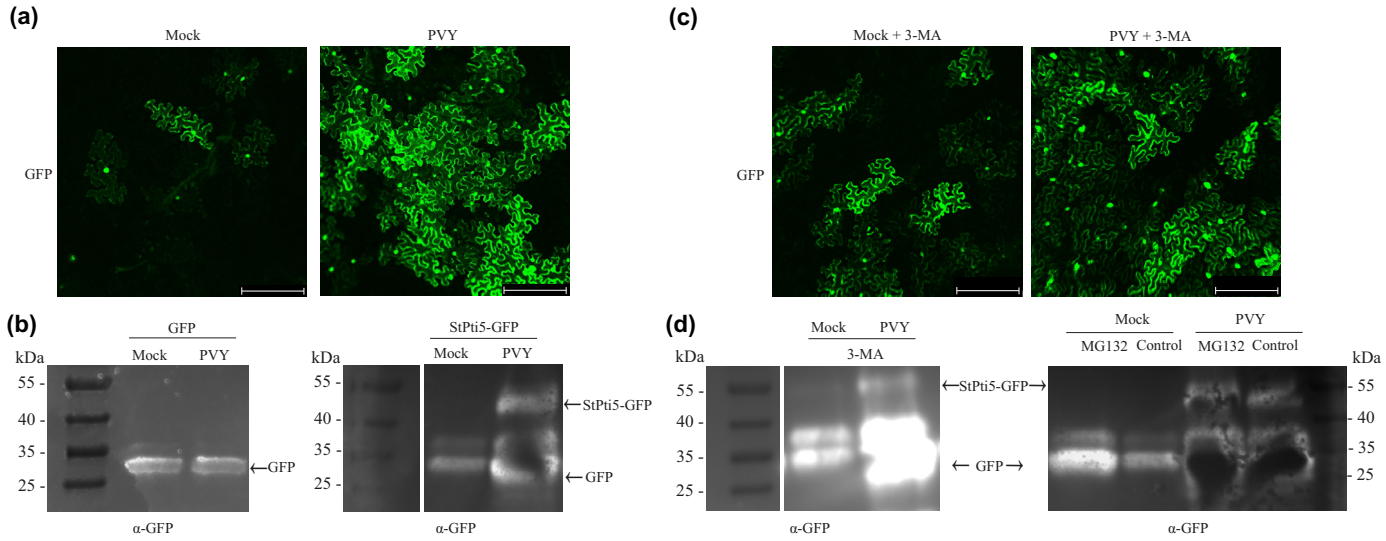

Fig. 7 Regulation of StPti5 protein accumulation during the immune response. (a) Localisation of the StPti5 protein in mock- (left) and PVY-inoculated leaves (right). Representative confocal microscopy images of *Nicotiana benthamiana* epidermal cells expressing StPti5-GFP under the β-estradiol inducible promoter (StPti5-GFP) are shown. Bar, 300 μm. StPti5-GFP and nucleus marker H2BRFP colocalisation, Chl channel and negative control are shown in Supporting Information Fig. S6. (b) western blot showing StPti5-GFP (47 kDa) and GFP (27 kDa) protein levels in mock- and PVY-infected plants infiltrated with *Agrobacterium* transformed with empty pABinGFP plasmid as a control (GFP; left) or StPti5 fused with GFP (StPti5-GFP; rig+ht). Anti-GFP antibodies (α-GFP) were used to detect the proteins. (c) Localisation of StPti5 in mock- (left) and PVY-inoculated leaves (right) treated with the autophagy inhibitor 3-methyladenine (3-MA). Representative confocal microscopy images of *N. benthamiana* epidermal cells expressing the StPti5-GFP protein are shown. Bar, 300 μm. (d) Levels of StPti5-GFP (47 kDa) and GFP (27 kDa) in mock- and PVY-infected plants treated with the 3-MA autophagy inhibitor (left), proteasome inhibitor (MG132; right) or with DMSO (control; right) were determined by immunoblot using anti-GFP antibodies (α-GFP). Protein size markers are indicated in kDa. Arrows indicate the target proteins StPti5-GFP and GFP. For full experimental details see Dataset S3 and for full western blot images Fig. S7.

(shPti5 NahG) plants in the early stage of infection (3 dpi). Using stringent analysis, we identified 19 genes that were significantly upregulated in the shStPti5 NahG line, while two showed significantly lower expression in these plants (Tables 1, S5, GSE136877). Such small differences were indeed expected due to the short time after PVY inoculation, by which the virus had just started multiplication (Lukan *et al.*, 2018a), and therefore, the StPti5 protein was accumulating in only a few cells. The results from this comparative analysis were validated by quantitative polymerase chain reaction (Fig. S8).

Among the genes upregulated in *StPti5*-silenced plants, five are potentially implicated in ubiquitin-related protein degradation mechanisms, the two F-box family proteins, two RING finger proteins, and *BTB-POZ domain-containing protein* (*StBTP-POZ*). Moreover, three proteases including *nepenthesin-1 aspartic proteinase*, *cathepsin L-like cysteine proteinase* and *eukaryotic aspartyl protease family protein* were found to be upregulated in *StPti5*-silenced plants. Interestingly, most of these protein degradation-related genes were significantly downregulated in the PVY-infected as compared with the mock-inoculated NahG plants, suggesting they are involved in potato–PVY interaction (Table S5).

Significant changes in gene expression were also observed in *StPti5*-silenced plants for three AP2/ERF family genes. *StERF51* and *StERF156* were shown to be upregulated in *StPti5*-silenced plants, while *StPti6* was significantly downregulated in *StPti5*-silenced plants, consistent with members of this gene family comprising a complex cross-regulatory network. Additionally, a *histidine phosphotransfer protein* with a role in cytokinin signalling was downregulated in shPti5 NahG plants.

Discussion

In this study, we showed that *StPti5*, a member of the ERF TF family, is a susceptibility (S) factor negatively regulating potato immunity to the viral pathogen PVY as well as the causal agent of bacterial wilt *R. solanacearum*.

One of the major mechanisms by which S factors facilitate susceptibility is via genes encoding negative regulators of immune signalling, including several TFs (Van Schie & Takken, 2014; Feng *et al.*, 2020). Like StPti5 (Fig. 4), some of the previously reported defence-suppressing TFs are also transcriptional activators. For example, AtWRKY38 and AtWRKY62, that compromise basal defence and increase susceptibility of Arabidopsis plants to *P. syringae* (Kim *et al.*, 2008), SlERF84 that negatively regulates immune response of tomato to *P. syringae* (Li *et al.*, 2018) and AtERF19, a negative regulator of PTI against *Botrytis cinerea* and *P. syringae* (Huang *et al.*, 2019), were all found to act as positive regulators of gene expression.

Pti5 was first identified in tomato as an interacting partner of the R *Pto* gene, encoding a serine/threonine kinase that confers resistance against the bacterial pathogen *P. syringae* pv tomato (Zhou *et al.*, 1997). Since then, its role in *Pto*-mediated resistance

Table 1 Differentially expressed genes in *StPti5*-silenced NahG vs NahG potato plants after PVY infection.

Function	ID	shPti5 NahG vs NahG (+ PVY) logFC	Description
Protein homeostasis	Sotub07g015000	2.89	Cathepsin L-like cysteine proteinase
	Sotub01g023000	2.40	Eukaryotic aspartyl protease family protein
	Sotub04g029470	2.22	Aspartic proteinase nepenthesin-1
	Sotub10g009090	3.68	RING finger protein 5 **(StRINF5)**
	Sotub11g012720	1.74	Ring finger protein
	Sotub01g009740	3.34	F-box family protein
	Sotub03g023340	1.98	BTB/POZ domain-containing protein **(StBTP-POZ)**
	Sotub11g025480	2.08	F-box family protein
Ethylene response factor	Sotub08g009520	1.96	Ethylene-responsive transcription factor 2b **(StERF156)**
	Sotub06g033380	−1.63	Ethylene-responsive transcription factor 1b **(StPti6)**
	Sotub12g018740	2.40	Ethylene-responsive transcription factor 1a **(StERF51)**
Other	Sotub08g015710	−2.06	Histidine phosphotransfer protein
	Sotub06g022940	4.44	Oxidative stress
	Sotub03g035870	3.42	Oxidative stress
	Sotub07g027860	1.75	Chaperone protein dnaJ 11
Unknown	Sotub06g006790	3.22	Protein of unknown function DUF506
	Sotub10g017020	1.69	Unknown Protein
	Sotub10g017040	1.67	Unknown Protein
	PGSC0003DMG400013938	1.93	Gene of unknown function
	Sotub10g011090	2.19	Unknown Protein
	Sotub12g007440	3.07	NHL repeat-containing protein

The intersection of genes obtained by two different statistical approaches using FDR-adjusted *P*-value < 0.05 as a cut-off is shown, grouped by their function. For each gene, identifier, $\log_2$FC (blue, downregulated; red, upregulated) and description are shown. shPti5 NahG: *StPti5*-silenced NahG. Gene short names used in this paper are marked in bold. Additional information on gene expression and function is presented in Supporting Information Table S5.

has been extensively studied (Zhou *et al.*, 1997; Thara *et al.*, 1999; He *et al.*, 2001; Wang *et al.*, 2021). SlPti5 was found to enhance resistance to aphids (*M. euphorbiae*) (Wu *et al.*, 2015) and *B. cinerea* in tomato (Qiong *et al.*, 2022), while Arabidopsis plants expressing this gene failed to show enhanced tolerance to the biotrophic fungal pathogen *Erysiphe orontii* or to the bacterial pathogen, *P. syringae* strain DC3000 (Gu *et al.*, 2002). Here we demonstrated a different role of StPti5 in potato immunity and proved that StPti5 negatively regulates plant immunity (Figs 2, 3). Similarly, the potato orthologue of the tomato transcriptional activator Pti4 was found to be an indispensable element of a repressosome complex (González-Lamothe *et al.*, 2008). These are examples of how evolutionary close genes can diverge in their function and represent an additional exception to the orthology–function conjecture (Gabaldon & Koonin, 2017).

Silencing the *StPti5* gene in an SA-deficient potato background, allowed us to analyse whether this factor enhanced or reduced plant susceptibility (nontransgenic plants are resistant to PVY and thus silencing *StPti5* would result in no phenotypic differences). We observed that StPti5 increased plant susceptibility to two pathogens with completely different modes of action (Figs 2, 3). PVY is a virus transmitted by aphids feeding on an infected leaf. Once in the new host, the virus must hijack the plant cell molecular machinery to complete its infectious cycle (Lacomme & Jacquot, 2017). By contrast, *R. solanacearum* is a soil-borne pathogen that thrives in the xylem vessels, and systemically spreads from there through the host plant (Planas-Marquès *et al.*, 2020; Xue *et al.*, 2020). To enhance potato susceptibility to such different types of pathogens, StPti5 might perturb pathways involved in immunity to a broad spectrum of pathogens. Several protein degradation pathway genes were found to be indirect downstream targets of StPti5 (Table 1). Higher expression of these genes in *StPti5*-silenced plants most likely leads to a more efficient immune response. It is well known that

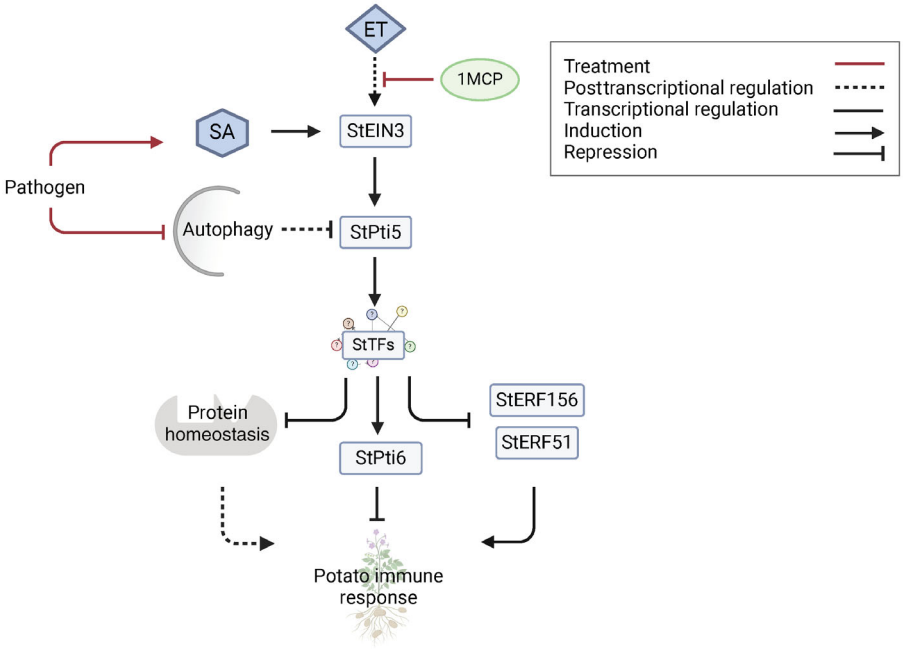

Fig. 8 Current knowledge-based scheme of StPit5 mode of action. Molecular events involved in up- and downstream regulation of StPti5 after pathogen attack are shown. PVY, potato virus Y; Ralstonia, *Ralstonia solanacearum*; SA, salicylic acid; ET, ethylene; 1MCP, 1-Methylcyclopropene; StEIN3, *ETHYLENE INSENSITIVE 3*; StTFs, unknown transcription factors; ERF, ethylene response factor. Red solid line: treatment; black solid line: transcriptional regulation; black dashed line: post-transcriptional regulation; arrow: induction; bar-headed arrow: repression. Created with BioRender.com.

ubiquitination has a central role in defence, with previous findings already demonstrating that it positively regulates plant immunity by promoting degradation of different negative immune regulators (Gao *et al.*, 2022). For example, the plant U-box type PUB17 increases potato resistance to *P. infestans* by targeting the putative K-homology RNA-binding protein for proteasome mediated degradation (McLellan *et al.*, 2020), while the BTB/ Pox virus and Zinc finger (POZ) enhances soybean resistance to *P. sojae*, by promoting the ubiquitination of the soybean AP2/ERF TF GmAP2 (Zhang *et al.*, 2021). Similarly, we hypothesise that the E3 ligases, indirectly regulated by StPti5 (Table 1), may be targeting further negative regulators of the immune response for degradation (Fig. 8).

According to our RNA-Seq data (Table 1), StPti5 acts also by indirectly repressing other AP2/ERF family members that are positive regulators of plant immunity (Fig. 8). In particular, *StERF156* whose orthologue *AtERF61* is induced in response to defence elicitors (Libault *et al.*, 2007) and *StERF51*, an orthologue of *AtERF105* with a positive role in Arabidopsis immunity against *P. syringae* (Cao *et al.*, 2019) were in our dataset induced in PVY-infected *StPti5*-silenced plants (Table 1). These are, however, not the only means of regulation of these genes as we have shown that *StERF51* is also repressed by ethylene treatment alone while the SA does not activate the expression of *StPti6* (Fig. S9).

Here we showed that *StPti5* expression is modulated at the transcriptional level by the ethylene and SA signalling pathways (Fig. 8). Our INA treatment results corroborate earlier findings (Wiesel *et al.*, 2015) showing that *StPti5* expression is induced by SA treatment (Fig. 6). Moreover, we here showed that active ethylene signalling is required for transcriptional *StPti5* regulation by SA (Fig. 6). We, in addition, demonstrated that StEIN3 and StEIL1, the potato orthologues of Arabidopsis, activate *StPti5* expression by directly binding to its promoter (Fig. 5), linking transcriptional *StPti5* control with the ethylene signalling pathway. Consistent with our data, several ERF TFs were reported to act downstream of EIN3 in the ethylene signalling cascade and be involved in plant defence responses against biotic and abiotic stresses (Zhang *et al.*, 2016; Huang *et al.*, 2021). By contrast, tomato *SlPti5* does not respond to ethylene, JA or SA treatments (Thara *et al.*, 1999), evidencing that the regulation of these two gene orthologues has evolutionarily diverged. Interestingly, despite the induction of StPti5 during the PVY infection (Fig. 1) and SA treatment (Fig. 6), the contribution of the suppression is not sufficient to break the resistance of potato to pathogens.

Hormone crosstalk is a crucial regulatory mechanism of plant immunity (Aerts *et al.*, 2021). The best characterised example of hormone–plant defence crosstalk interaction is the antagonism between the JA/ethylene and SA pathways (Van der Does *et al.*, 2013; Caarls *et al.*, 2016; He *et al.*, 2017). Many examples of synergism between SA and ethylene modules have also been reported. For instance, potentiation of SA-dependent immune response by ethylene has been previously described in Arabidopsis (Leon-Reyes *et al.*, 2009) and potato (Ramšak *et al.*, 2018). Moreover, a requirement of SA for ethylene-dependent gene expression was also unveiled in studies where SA application enhanced EIN3 protein abundance and activated the ethylene signalling pathway (He *et al.*, 2017). A similar SA and ethylene cross-regulation may also explain *StPti5* induction in SA-deficient NahG plants after viral infection (Fig. 1).

The activity of TFs must be tightly regulated since transcriptional reprogramming is crucial for an efficient immune response. Therefore, it is not surprising that immunity-related TFs are subjected to different levels of regulation to fine-tune their activity. For instance, AtTGA3, a member of the TGACG-binding (TGA) family, is modulated at transcriptional (Winter *et al.*, 2007) and protein stability levels (Pontier *et al.*, 2002), in

addition to the protein–protein interaction control (Tomaž *et al.*, 2022). On the other hand, StERF6 involved in defence response to *B. cinerea*, is regulated at transcriptional and posttranslational levels by MPK3/MPK6 (Meng *et al.*, 2013). Moreover, Wang *et al.* (2021) recently reported that SlPti5 might be regulated in tomato, not only at transcriptional level but also at the protein level through the 26S proteasome pathway. Similarly, we here observed that StPti5 is regulated at transcriptional and protein stability levels. At the transcriptional level, *StPti5* gene expression is regulated by ethylene-SA crosstalk, while at the protein level, StPti5 stability is regulated through autophagy (Fig. 8) and not proteasomal pathway.

The dualistic function of autophagy in plant immunity is becoming evident (Leary *et al.*, 2019; Sertsuvalkul *et al.*, 2022). This cellular process plays a crucial role in defence response against pathogens, yet, microbes can in turn manipulate autophagy for their own benefit (Yang & Liu, 2022). Several reports have now shown that viruses target plant defence factors for degradation, by hijacking autophagy. For example, the P0 protein from turnip yellow virus activates the ER-autophagy pathway to induce degradation of the RNA silencing component argonaute 1 (Michaeli *et al.*, 2019), while the VPg protein from this virus targets the antiviral protein SGS3 to degradation through both 20S ubiquitin-proteasome and autophagy pathways (Cheng & Wang, 2017). We hypothesise that pathogens might hamper StPti5 degradation by manipulating autophagy and thus allow this susceptible factor to perturb immune responses and facilitate pathogen infection. Despite its function as a negative regulator of plant immunity, we should not neglect other beneficial effects that StPti5 must have, otherwise function of this gene would have been lost during evolution.

In conclusion, we here show that StPti5 is a susceptibility factor that attenuates the potato defence response to two pathogens with completely different modes of action, probably by perturbing the protein degradation pathway involved in general immunity. Through this, we proved a different role of StPti5 compared with its orthologue in tomato, which entails a further exception for the orthology–function conjecture.

Acknowledgements

We thank Prof. Andrej Blejec for help with statistical analysis; Lidija Matičič, Dr Maruša Pompe Novak, Maja Križnik, Dr David Dobnik, Katja Fric, Valentina Levak, Nastja Marondini and Dr Špela Tomaž for technical support and laboratory assistance. This research was financially supported by the Slovenian Research Agency (research core funding no. P4-0165 and projects J1-4268, J4-7636, J4-1777 and J1-2467) and The European Cooperation in Science and Technology (FA1405 and CA15223 COST Actions).

Competing interests

None declared.

Author contributions

KG and AC designed the research; TL, KS, TMP and AC performed the research; MZ and SB contributed with new analytic/-computational tools; MZ, MP, SP, NSC, MV, KG and AC analysed the data; TL, KS, SP, NSC, MV, MZ, MP, SB, TMP, KG and AC contributed to the writing or revision of the article.

ORCID

Špela Baebler https://orcid.org/0000-0003-4776-7164
Anna Coll https://orcid.org/0000-0003-0672-1530
Núria Sánchez Coll https://orcid.org/0000-0002-8889-0399
Kristina Gruden https://orcid.org/0000-0001-5906-8569
Tjaša Lukan https://orcid.org/0000-0002-6235-2816
Tjaša Mahkovec Povalej https://orcid.org/0000-0003-3706-2371
Marko Petek https://orcid.org/0000-0003-3644-7827
Salomé Prat https://orcid.org/0000-0003-2684-5485
Katja Stare https://orcid.org/0000-0002-3999-9400
Marc Valls https://orcid.org/0000-0003-2312-0091
Maja Zagorščak https://orcid.org/0000-0002-1669-6482

Data availability

The raw data and counts table were deposited to the Gene Expression Omnibus (GEO) and are available under accession no. GSE136877. Sequence data from this article can be found in the GenBank data library under accession nos.: *NAC domain-containing protein 55* (*StANAC55*, GenBank: OR736059), *MYC2 transcription factor* (*StMYC*, GenBank: OR736060), *EIN3-like 1* (*StEIL1*, GenBank: OR736061), *EIN3-like 2 (StEIL2*, GenBank: OR736062).

References

Aerts N, Pereira Mendes M, Van Wees SCM. 2021. Multiple levels of crosstalk in hormone networks regulating plant defense. *The Plant Journal* **105**: 489–504.

Allen MD, Yamasaki K, Ohme-Takagi M, Tateno M, Suzuki M. 1998. A novel mode of DNA recognition by a beta-sheet revealed by the solution structure of the GCC-box binding domain in complex with DNA. *EMBO Journal* **17**: 5484–5496.

Baebler Š, Krečič-Stres H, Rotter A, KogovŠek P, Cankar K, Kok EJ, Gruden K, KovaČ M, Žel J, Pompe-Novak M *et al.* 2009. PVYNTN elicits a diverse gene expression response in different potato genotypes in the first 12 h after inoculation. *Molecular Plant Pathology* **10**: 263–275.

Baebler Š, Svalina M, Petek M, Stare K, Rotter A, Pompe-Novak M, Gruden K. 2017. quantGenius: implementation of a decision support system for qPCR-based gene quantification. *BMC Bioinformatics* **18**: 276.

Baebler Š, Witek K, Petek M, Stare K, Tušek-Žnidarič M, Pompe-Novak M, Renaut J, Szajko K, Strzelczyk-Zyta D, Marczewski W *et al.* 2014. Salicylic acid is an indispensable component of the Ny-1 resistance-gene-mediated response against Potato virus Y infection in potato. *Journal of Experimental Botany* **65**: 1095–1109.

Berrocal-Lobo M, Molina A. 2004. Ethylene response factor 1 mediates Arabidopsis resistance to the soilborne fungus *Fusarium oxysporum*. *Molecular Plant–Microbe Interactions* **17**: 763–770.

Berrocal-Lobo M, Molina A, Solano R. 2002. Constitutive expression of ETHYLENE-RESPONSE-FACTOR1 in Arabidopsis confers resistance to several necrotrophic fungi. *The Plant Journal* **29**: 23–32.

Birkenbihl RP, Liu S, Somssich IE. 2017. Transcriptional events defining plant immune responses. *Current Opinion in Plant Biology* **38**: 1–9.

Bleckmann A, Weidtkamp-Peters S, Seidel CAM, Simon R. 2010. Stem cell signaling in Arabidopsis requires CRN to localize CLV2 to the plasma membrane. *Plant Physiology* **152**: 166–176.

Bodenhofer U, Kothmeier A, Hochreiter S. 2011. APCLUSTER: an R package for affinity propagation clustering. *Bioinformatics* **27**: 2463–2464.

Boller T, Felix G. 2009. A renaissance of elicitors: perception of microbe-associated molecular patterns and danger signals by pattern-recognition receptors. *Annual Review of Plant Biology* **60**: 379–406.

Caarls L, Van der Does D, Hickman R, Jansen W, Van Verk MC, Proietti S, Lorenzo O, Solano R, Pieterse CMJ, Van Wees SCM. 2016. Assessing the role of ETHYLENE RESPONSE FACTOR transcriptional repressors in salicylic acid-mediated suppression of jasmonic acid-responsive genes. *Plant and Cell Physiology* **108**: pcw187.

Cao FY, Khan M, Taniguchi M, Mirmiran A, Moeder W, Lumba S, Yoshioka K, Desveaux D. 2019. A host–pathogen interactome uncovers phytopathogenic strategies to manipulate plant ABA responses. *The Plant Journal* **100**: 187–198.

Charfeddine M, Saïdi MN, Charfeddine S, Hammami A, Gargouri Bouzid R. 2014. Genome-wide analysis and expression profiling of the ERF transcription factor family in potato (*Solanum tuberosum* L.). *Molecular Biotechnology* **57**: 348–358.

Cheng X, Wang A. 2017. The potyvirus silencing suppressor protein VPg mediates degradation of SGS3 via ubiquitination and autophagy pathways. *Journal of Virology* **91**: e01478-16.

Cruz APZ, Ferreira V, Pianzzola MJ, Siri MI, Coll NS, Valls M. 2014. A novel, sensitive method to evaluate potato germplasm for bacterial wilt resistance using a luminescent *Ralstonia solanacearum* reporter strain. *Molecular Plant–Microbe Interactions* **27**: 277–285.

Cui H, Tsuda K, Parker JE. 2015. Effector-triggered immunity: from pathogen perception to robust defense. *Annual Review of Plant Biology* **66**: 487–511.

Dolničar P. 2021. Importance of potato as a crop and practical approaches to potato breeding. In: Dobnik D, Gruden K, Ramšak Ž, Coll A, eds. *Solanum tuberosum*: Methods and Protocols. New York, NY, USA: Humana Press, 3–20.

Dong L, Cheng Y, Wu J, Cheng Q, Li W, Fan S, Jiang L, Xu Z, Kong F, Zhang D *et al.* 2015. Overexpression of GmERF5, a new member of the soybean EAR motif-containing ERF transcription factor, enhances resistance to *Phytophthora sojae* in soybean. *Journal of Experimental Botany* **66**: 2635–2647.

Feng K, Hou XL, Xing GM, Liu JX, Duan AQ, Xu ZS, Li MY, Zhuang J, Xiong AS. 2020. Advances in AP2/ERF super-family transcription factors in plant. *Critical Reviews in Biotechnology* **40**: 750–776.

Gabaldon T, Koonin EV. 2017. Functional and evolutionary implications of gene orthology. *Nature Reviews Genetics* **176**: 139–148.

Galili T. 2015. DENDEXTEND: an R package for visualizing, adjusting and comparing trees of hierarchical clustering. *Bioinformatics* **31**: 3718–3720.

Gao C, Tang D, Wang W. 2022. The role of ubiquitination in plant immunity: fine-tuning immune signaling and beyond. *Plant and Cell Physiology* **63**: 1405–1413.

González-Lamothe R, Boyle P, Dulude A, Roy V, Lezin-Doumbou C, Kaur GS, Bouarab K, Despres C, Brisson N. 2008. The transcriptional activator Pti4 is required for the recruitment of a repressosome nucleated by repressor SEBF at the potato PR-10a gene. *Plant Cell* **20**: 3136–3147.

Gu YQ, Wildermuth MC, Chakravarthy S, Loh YT, Yang C, He X, Han Y, Martin GB. 2002. Tomato transcription factors Pti4, Pti5, and Pti6 activate defense responses when expressed in Arabidopsis. *Plant Cell* **14**: 817–831.

He P, Warren RF, Zhao T, Shan L, Zhu L, Tang X, Zhou JM. 2001. Overexpression of Pti5 in tomato potentiates pathogen-induced defense gene expression and enhances disease resistance to *Pseudomonas syringae* pv. tomato. *Molecular Plant–Microbe Interactions* **14**: 1453–1457.

He X, Jiang J, Wang CQ, Dehesh K. 2017. ORA59 and EIN3 interaction couples jasmonate-ethylene synergistic action to antagonistic salicylic acid regulation of PDF expression. *Journal of Integrative Plant Biology* **59**: 275–287.

Huang J, Zhao X, Bürger M, Wang Y, Chory J. 2021. Two interacting ethylene response factors regulate heat stress response. *Plant Cell* **33**: 338–357.

Huang P, Catinot J, Zimmerli L. 2015. Ethylene response factors in Arabidopsis immunity. *Journal of Experimental Botany* **67**: 1231–1241.

Huang PY, Zhang J, Jiang B, Chan C, Yu JH, Lu YP, Chung KM, Zimmerli L. 2019. NINJA-associated ERF19 negatively regulates Arabidopsis pattern-triggered immunity. *Journal of Experimental Botany* **70**: 739–745.

Jakab G, Droz E, Brigneti G, Baulcombe D, Malnoë P. 1997. Infectious *in vivo* and *in vitro* transcripts from a full-length cDNA clone of PVY-N605, a Swiss necrotic isolate of potato virus Y. *Journal of General Virology* **78**: 3141–3145.

Karimi M, Inzé D, Depicker A. 2002. GATEWAY™ vectors for Agrobacterium-mediated plant transformation. *Trends in Plant Science* **7**: 193–195.

Kassambara A. 2023a. *RSTATIX: pipe-friendly framework for basic statistical tests.* R package v.0.7.2. [WWW document] URL https://CRAN.R-project.org/package=rstatix.

Kassambara A. 2023b. *GGPUBR: 'GGPLOT2' based publication ready plots.* R package v.0.6.0. [WWW document] URL https://CRAN.R-project.org/package=ggpubr.

Kim KC, Lai Z, Fan B, Chen Z. 2008. Arabidopsis WRKY38 and WRKY62 transcription factors interact with histone deacetylase 19 in basal defense. *Plant Cell* **20**: 2357–2371.

Kloosterman B, De Koeyer D, Griffiths R, Flinn B, Steuernagel B, Scholz U, Sonnewald S, Sonnewald U, Bryan GJ, Prat S *et al.* 2008. Genes driving potato tuber initiation and growth: identification based on transcriptional changes using the POCI array. *Functional & Integrative Genomics* **8**: 329–340.

Kreuze JF, Jeevalatha A, Figueira AR. 2020. Viral diseases in potato. In: Campos H, Ortiz O, eds. *The potato crop*. Cham, Switzerland: Springer, 389–430.

Lacomme C, Jacquot E. 2017. General characteristics of potato virus Y (PVY) and its impact on potato production: an overview. In: Lacomme C, Glais L, Bellstedt DU, Dupuis B, Karasev AV, Jacquot E, eds. *Potato virus Y: biodiversity, pathogenicity, epidemiology and management*. Cham, Switzerland: Springer, 1–19.

Lasierra P, Prat S. 2018. Transient transactivation studies in *Nicotiana benthamiana* leaves. In: Oñate-Sánchez L, ed. *Two-hybrid systems*. New York, NY, USA: Humana Press, 311–322.

Leary AY, Savage Z, Tumtas Y, Bozkurt TO. 2019. Contrasting and emerging roles of autophagy in plant immunity. *Current Opinion in Plant Biology* **52**: 46–53.

Leon-Reyes A, Spoel SH, De Lange ES, Abe H, Kobayashi M, Tsuda S, Millenaar FF, Welschen RAM, Ritsema T, Pieterse CMJ. 2009. Ethylene modulates the role of NONEXPRESSOR OF PATHOGENESIS-RELATED GENES1 in cross talk between salicylate and jasmonate signaling. *Plant Physiology* **149**: 1797–1809.

Li N, Niu Y, Wang X, Wang S, Chen Y, Wang L. 2023. A novel eggplant AP2/ERF transcription factor StPti5 confers resistance to Verticillium wilt across different species. *Plant Protection Science* **59**: 325–336.

Li Z, Tian Y, Xu J, Fu X, Gao J, Wang B, Han H, Wang L, Peng R, Yao Q. 2018. A tomato ERF transcription factor, SlERF84, confers enhanced tolerance to drought and salt stress but negatively regulates immunity against *Pseudomonas syringae* pv. *tomato* DC3000. *Plant Physiology and Biochemistry* **132**: 683–695.

Libault M, Wan J, Czechowski T, Udvardi M, Stacey G. 2007. Identification of 118 Arabidopsis transcription factor and 30 ubiquitin-ligase genes responding to chitin, a plant-defense elicitor. *Molecular Plant–Microbe Interactions* **20**: 900–911.

Liu D, Chen X, Liu J, Ye J, Guo Z. 2012. The rice ERF transcription factor OsERF922 negatively regulates resistance to *Magnaporthe oryzae* and salt tolerance. *Journal of Experimental Botany* **63**: 695–709.

van der Loo MPJ. 2014. The STRINGDIST package for approximate string matching. *R Journal* **6**: 111–122.

Lorenzo O, Piqueras R, Sánchez-serrano JJ, Solano R. 2003. ETHYLENE RESPONSE FACTOR1 integrates signals from ethylene and jasmonate pathways in plant defense. *Plant Cell* **15**: 165–178.

Lukan T, Baebler Š, Pompe-Novak M, Guček K, Zagorščak M, Coll A, Gruden K. 2018a. Cell death is not sufficient for the restriction of potato virus Y spread in hypersensitive response-conferred resistance in potato. *Frontiers in Plant Science* **9**: 168.

Lukan T, Machens F, Coll A, Baebler Š, Messerschmidt K, Gruden K. 2018b. Plant X-tender: an extension of the AssemblX system for the assembly and expression of multigene constructs in plants. *PLoS ONE* **13**: e0190526.

Lukan T, Pompe-Novak M, Baebler Š, Tušek-Žnidarič M, Kladnik A, Križnik M, Blejec A, Zagorščak M, Stare K, Dušak B *et al.* 2020. Precision transcriptomics of viral foci reveals the spatial regulation of immune-signaling genes and identifies RBOHD as an important player in the incompatible interaction between potato virus Y and potato. *The Plant Journal* **104**: 645–661.

Lukan T, Županič A, Mahkovec Povalej T, Brunkard JO, Kmetič M, Juteršek M, Baebler Š, Gruden K. 2023. Chloroplast redox state changes mark cell-to-cell signaling in the hypersensitive response. *New Phytologist* **237**: 548–562.

Mansfield J, Genin S, Magori S, Citovsky V, Sriariyanum M, Ronald P, Dow M, Verdier V, Beer SV, Machado MA *et al.* 2012. Top 10 plant pathogenic bacteria in molecular plant pathology. *Molecular Plant Pathology* **13**: 614–629.

McLellan H, Chen K, He Q, Wu X, Boevink PC, Tian Z, Birch PRJ. 2020. The ubiquitin E3 ligase PUB17 positively regulates immunity by targeting a negative regulator, KH17, for degradation. *Plant Communications* **1**: 100020.

Meng X, Xu J, He Y, Yang K-Y, Mordorski B, Liu Y, Zhang S. 2013. Phosphorylation of an ERF transcription factor by Arabidopsis MPK3/MPK6 regulates plant defense gene induction and fungal resistance. *Plant Cell* **25**: 1126–1142.

Michaeli S, Clavel M, Lechner E, Viotti C, Wu J, Dubois M, Hacquard T, Derrien B, Izquierdo E, Lecorbeiller M *et al.* 2019. The viral F-box protein P0 induces an ER-derived autophagy degradation pathway for the clearance of membrane-bound AGO1. *Proceedings of the National Academy of Sciences, USA* **116**: 22872–22883.

Nakagawa T, Suzuki T, Murata S, Nakamura S, Hino T, Maeo K, Tabata R, Kawai T, Tanaka K, Niwa Y *et al.* 2007. Improved gateway binary vectors: high-performance vectors for creation of fusion constructs in transgenic analysis of plants. *Bioscience, Biotechnology and Biochemistry* **71**: 2095–2100.

Nakano T, Suzuki K, Fujimura T, Shinshi H. 2006. Genome-wide analysis of the ERF gene family. *Plant Physiology* **140**: 411–432.

Ngou BPM, Ahn HK, Ding P, Jones JDG. 2021. Mutual potentiation of plant immunity by cell-surface and intracellular receptors. *Nature* **592**: 110–115.

Ohme-Takagi M, Shinshi H. 1995. Ethylene-Inducible DNA binding proteins that interact with an ethylene-responsive element. *Plant Cell* **7**: 173–182.

Ow DW, Jacobst JD, Howell SH. 1987. Functional regions of the cauliflower mosaic virus 35S RNA promoter determined by use of the firefly luciferase gene as a reporter of promoter activity. *Biochemistry* **84**: 4870–4874.

de Pedro-Jové R, Puigvert M, Sebastià P, Macho AP, Monteiro JS, Coll NS, Setúbal JC, Valls M. 2021. Dynamic expression of *Ralstonia solanacearum* virulence factors and metabolism-controlling genes during plant infection. *BMC Genomics* **22**: 1–18.

Pirrello J, Prasad BCN, Zhang W, Chen K, Mila I, Zouine M, Latché A, Pech JC, Ohme-Takagi M, Regad F *et al.* 2012. Functional analysis and binding affinity of tomato ethylene response factors provide insight on the molecular bases of plant differential responses to ethylene. *BMC Plant Biology* **12**: 190.

Planas-Marquès M, Kressin JP, Kashyap A, Panthee DR, Louws FJ, Coll NS, Valls M. 2020. Four bottlenecks restrict colonization and invasion by the pathogen *Ralstonia solanacearum* in resistant tomato. *Journal of Experimental Botany* **71**: 2157–2171.

Pontier D, Privat I, Trifa Y, Zhou JM, Klessig DF, Lam E. 2002. Differential regulation of TGA transcription factors by post-transcriptional control. *The Plant Journal* **32**: 641–653.

Potato Genome Sequencing Consortium. 2011. Genome sequence and analysis of the tuber crop potato. *Nature* **475**: 189–195.

Pré M, Atallah M, Champion A, De Vos M, Pieterse CMJ, Memelink J. 2008. The AP2/ERF domain transcription factor ORA59 integrates jasmonic acid and ethylene signals in plant defense. *Plant Physiology* **147**: 1347–1357.

Qiong T, Xiao Dong Z, Jun G, Ting Y. 2022. Tomato SlPti5 plays a regulative role in the plant immune response against *Botrytis cinerea* through modulation of ROS system and hormone pathways. *Journal of Integrative Agriculture* **21**: 697–709.

R Core Team. 2023. *R: a language and environment for statistical computing.* Vienna, Austria: R Foundation for Statistical Computing. [WWW document] URL https://www.R-project.org.

Ramšak Z, Baebler S, Rotter A, Korbar M, Mozetic I, Usadel B, Gruden K. 2013. GoMapMan: integration, consolidation and visualization of plant gene annotations within the MapMan ontology. *Nucleic Acids Research* **42**: 1–9.

Ramšak Ž, Coll A, Stare T, Tzfadia O, Baebler Š, Van de Peer Y, Gruden K. 2018. Network modelling unravels mechanisms of crosstalk between ethylene and salicylate signalling in potato. *Plant Physiology* **178**: 488–499.

Sakuma Y, Liu Q, Dubouzet JG, Abe H, Shinozaki K, Yamaguchi-Shinozaki K. 2002. DNA-binding specificity of the ERF/AP2 domain of Arabidopsis DREBs, transcription factors involved in dehydration- and cold-inducible gene expression. *Biochemical and Biophysical Research Communications* **290**: 998–1009.

Sanger F, Nicklen S, Coulson AR. 1977. DNA sequencing with chain-terminating inhibitors. *Proceedings of the National Academy of Sciences, USA* **74**: 5463–5467.

Sebastian A, Contreras-Moreira B. 2014. FootprintDB: a database of transcription factors with annotated cis elements and binding interfaces. *Bioinformatics* **30**: 258–265.

Sertsuvalkul N, DeMell A, Dinesh-Kumar SP. 2022. The complex roles of autophagy in plant immunity. *FEBS Letters* **596**: 2163–2171.

Sharma MK, Kumar R, Solanke AU, Sharma R, Tyagi AK, Sharma AK. 2010. Identification, phylogeny, and transcript profiling of ERF family genes during development and abiotic stress treatments in tomato. *Molecular Genetics and Genomics* **284**: 455–475.

Smith LM, Sanders JZ, Kaiser RJ, Hughes P, Dodd C, Connell CR, Heiner C, Kent SBH, Hood LE. 1986. Fluorescence detection in automated DNA sequence analysis. *Nature* **321**: 674–679.

Thara V, Tang X, Gu Y, Martin G, Zhou J. 1999. Pseudomonas syringae pv tomato induces the expression of tomato EREBP-like genes pti4 and pti5 independent of ethylene, salicylate and jasmonate. *The Plant Journal* **20**: 475–483.

The Tomato Genome Consortium. 2012. The tomato genome sequence provides insights into fleshy fruit evolution. *Nature* **485**: 635–641.

Tian Z, He Q, Wang H, Liu Y, Zhang Y, Shao F, Xie C. 2015. The potato ERF transcription factor StERF3 negatively regulates resistance to *Phytophthora infestans* and salt tolerance in potato. *Plant and Cell Physiology* **56**: 992–1005.

Tomaž Š, Gruden K, Coll A. 2022. TGA transcription factors—structural characteristics as basis for functional variability. *Frontiers in Plant Science* **13**: 1–12.

Tomaž Š, Petek M, Lukan T, Pogačar K, Stare K, Prates ET, Jacobson DA, Zrimec J, Bajc G, Butala M *et al.* 2023. A mini-TGA protein modulates gene expression through heterogeneous association with transcription factors. *Plant Physiology* **191**: 1934–1952.

Tsuda K, Somssich IE. 2015. Transcriptional networks in plant immunity. *New Phytologist* **206**: 932–947.

Van der Does D, Leon-Reyes A, Koornneef A, Van Verk MC, Rodenburg N, Pauwels L, Goossens A, Körbes AP, Memelink J, Ritsema T *et al.* 2013. Salicylic acid suppresses jasmonic acid signaling downstream of SCFCOI1-JAZ by targeting GCC promoter motifs via transcription factor ORA59. *Plant Cell* **25**: 744–761.

Van Schie CCN, Takken FLW. 2014. Susceptibility genes 101: how to be a good host. *Annual Review of Phytopathology* **52**: 551–581.

Wang Y, Feng G, Zhang Z, Liu Y, Ma Y, Wang Y, Ma F, Zhou Y, Gross R, Xu H *et al.* 2021. Overexpression of Pti4, Pti5, and Pti6 in tomato promote plant defense and fruit ripening. *Plant Science* **302**: 110702.

Wang Z, Zhang N, Zhou X, Fan Q, Si H, Wang D. 2015. Isolation and characterization of StERF transcription factor genes from potato (*Solanum tuberosum* L.). *Comptes Rendus – Biologies* **338**: 219–226.

Warnes G, Bolker B, Bonebakker L, Gentleman R, Huber W, Liaw A, Lumley T, Maechler M, Magnusson A, Moeller S *et al.* 2022. *gplots: various R programming tools for plotting data.* R package v.3.1.3. [WWW document] URL https://CRAN.R-project.org/package=gplots.

Wickham H. 2016. *ggplot2: elegant graphics for data analysis.* New York, NY, USA: Springer-Verlag.

Wiesel L, Davis JL, Milne L, Redondo Fernandez V, Herold MB, Middlefell Williams J, Morris J, Hedley PE, Harrower B, Newton AC *et al.* 2015. A transcriptional reference map of defence hormone responses in potato. *Scientific Reports* **5**: 15229.

Winter D, Vinegar B, Nahal H, Ammar R, Wilson GV, Provart NJ. 2007. An 'electronic fluorescent pictograph' browser for exploring and analyzing large-scale biological data sets. *PLoS ONE* **2**: 1–12.

Wu C, Avila CA, Goggin FL. 2015. The ethylene response factor Pti5 contributes to potato aphid resistance in tomato independent of ethylene signalling. *Journal of Experimental Botany* **66**: 559–570.

Xue H, Lozano-Duran R, Macho AP. 2020. Insights into the root invasion by the plant pathogenic bacterium *Ralstonia solanacearum*. *Plants* **9**: 516.

Yang M, Liu Y. 2022. Autophagy in plant viral infection. *FEBS Letters* **596**: 2152–2162.

Yuan M, Jiang Z, Bi G, Nomura K, Liu M, Wang Y, Cai B, Zhou JM, He SY, Xin XF. 2021a. Pattern-recognition receptors are required for NLR-mediated plant immunity. *Nature* **592**: 105–109.

Yuan M, Pok B, Ngou M, Ding P, Xin X. 2021b. PTI-ETI crosstalk: an integrative view of plant immunity. *Current Opinion in Plant Biology* **62**: 102030.

Zarei A, Körbes AP, Younessi P, Montiel G, Champion A, Memelink J. 2011. Two GCC boxes and AP2/ERF-domain transcription factor ORA59 in jasmonate/ethylene-mediated activation of the PDF1.2 promoter in Arabidopsis. *Plant Molecular Biology* **75**: 321–331.

Zhang C, Gao H, Sun Y, Jiang L, He S, Song B, Liu S, Zhao M, Wang L, Liu Y *et al.* 2021. The BTB/POZ domain protein GmBTB/POZ promotes the ubiquitination and degradation of the soybean AP2/ERF-like transcription factor GmAP2 to regulate the defense response to *Phytophthora sojae*. *Journal of Experimental Botany* **72**: 7891–7908.

Zhang H, Li A, Zhang Z, Huang Z, Lu P, Zhang D, Liu X, Zhang Z-F, Huang R. 2016. Ethylene response factor TERF1, regulated by ETHYLENE-INSENSITIVE3-like factors, functions in reactive oxygen species (ROS) scavenging in tobacco (*Nicotiana tabacum* L.). *Scientific Reports* **6**: 29948.

Zhao Y, Chang X, Qi D, Dong L, Wang G, Fan S, Jiang L, Cheng Q, Chen X, Han D *et al.* 2017. A novel soybean ERF transcription factor, GmERF113, increases resistance to *Phytophthora sojae* infection in soybean. *Frontiers in Plant Science* **8**: 1–16.

Zhou J, Tang X, Martin GB. 1997. The Pto kinase conferring resistance to tomato bacterial speck disease interacts with proteins that bind a *cis*-element of pathogenesis-related genes. *EMBO Journal* **16**: 3207–3218.

Zhou JM, Zhang Y. 2020. Plant immunity: danger perception and signaling. *Cell* **181**: 978–989.

Zhu Z, Shi J, Xu W, Li H, He M, Xu Y, Xu T, Yang Y, Cao J, Wang Y. 2013. Three ERF transcription factors from Chinese wild grapevine *Vitis pseudoreticulata* participate in different biotic and abiotic stress-responsive pathways. *Journal of Plant Physiology* **170**: 923–933.

Supporting Information

Additional Supporting Information may be found online in the Supporting Information section at the end of the article.

Dataset S1 Sample information for hormonal treatment experiments.

Dataset S2 Sample information for experiments that involved the use of *StPti5*-silenced NahG potato plants.

Dataset S3 Sample information for StPti5 localisation and regulation studies.

Dataset S4 Disease index of potato plants infected with *Ralstonia solanacearum*.

Dataset S5 Sequences of StPti5 promoter variants amplified from genomic DNA of nontransgenic (NT) potato plants used for *in silico* promoter analysis.

Fig. S1 Phylogenetic tree of ERF-IX subfamily from *Arabidopsis thaliana* (At), potato (Sotub) and tomato (Sl).

Fig. S2 Phenotype and silencing levels of short hairpin RNA (shRNA) potato plants.

Fig. S3 Symptom development on inoculated potato leaves from two independent experiments.

Fig. S4 Confirmation of expression of GFP-tagged genes under β-estradiol inducible promoter in *Nicotiana benthamiana* leaves.

Fig. S5 Hormonal regulation of Pti5 expression.

Fig. S6 Effect of proteasome inhibitor on StPti5 degradation.

Fig. S7 Full blot images, used for the preparation of Fig. 7(b,d).

Fig. S8 Validation of RNA-Seq data by quantitative polymerase chain reaction.

Fig. S9 Hormonal regulation of *StERF51* and *StPTI6* expression.

Methods S1 RNA-Seq analysis.

Methods S2 Western blot.

Methods S3 Confocal microscopy.

Table S1 Oligonucleotides used for cloning.

Table S2 Quantitative polymerase chain reaction assays used in this study (MIQE compliant).

Table S3 Transcription factor binding sites in StPti5 promoter variants.

Table S4 Relative amount of StPti5 mRNA in mock- and PVY-inoculated *Nicotiana benthamiana* leaves expressing translational fusion of StPti5 with GFP.

Table S5 Differential gene expression in *StPti5-silenced* NahG after PVY infection.

Please note: Wiley is not responsible for the content or functionality of any Supporting Information supplied by the authors. Any queries (other than missing material) should be directed to the *New Phytologist* Central Office.